Integrative taxonomy reveals three new species and one new record of *Psychropotes* (Holothuroidea, Elasipodida , Psychropotidae) from the Kermadec Trench region and the Wallaby-Zenith Fracture Zone (#105583)

First submission

Guidance from your Editor

Please submit by **1 Oct 2024** for the benefit of the authors (and your token reward) .

Structure and Criteria
Please read the 'Structure and Criteria' page for guidance.

Custom checks
Make sure you include the custom checks shown below, in your review.

Author notes
Have you read the author notes on the guidance page?

Raw data check
Review the raw data.

Image check
Check that figures and images have not been inappropriately manipulated.

If this article is published your review will be made public. You can choose whether to sign your review. If uploading a PDF please remove any identifiable information (if you want to remain anonymous).

Files

Download and review all files from the materials page.

16 Figure file(s)
2 Table file(s)
2 Other file(s)

Custom checks

DNA data checks

- Have you checked the authors data deposition statement?
- Can you access the deposited data?
- Has the data been deposited correctly?
- Is the deposition information noted in the manuscript?

Systematic review or meta analysis

- Have you checked our policies?

- Is the topic of the study relevant and meaningful?
- Are the results robust and believable?

New species checks

- Have you checked our new species policies?
- Do you agree that it is a new species?
- Is it correctly described e.g. meets ICZN standard?

For assistance email peer.review@peerj.com

Structure and Criteria

Structure your review

The review form is divided into 5 sections. Please consider these when composing your review:

1. **BASIC REPORTING**
2. **EXPERIMENTAL DESIGN**
3. **VALIDITY OF THE FINDINGS**
4. General comments
5. Confidential notes to the editor

You can also annotate this PDF and upload it as part of your review

When ready submit online.

Editorial Criteria

Use these criteria points to structure your review. The full detailed editorial criteria is on your guidance page.

BASIC REPORTING

- Clear, unambiguous, professional English language used throughout.
- Intro & background to show context. Literature well referenced & relevant.
- Structure conforms to PeerJ standards, discipline norm, or improved for clarity.
- Figures are relevant, high quality, well labelled & described.
- Raw data supplied (see PeerJ policy).

EXPERIMENTAL DESIGN

- Original primary research within Scope of the journal.
- Research question well defined, relevant & meaningful. It is stated how the research fills an identified knowledge gap.
- Rigorous investigation performed to a high technical & ethical standard.
- Methods described with sufficient detail & information to replicate.

VALIDITY OF THE FINDINGS

- **Impact and novelty is not assessed.** Meaningful replication encouraged where rationale & benefit to literature is clearly stated.
- All underlying data have been provided; they are robust, statistically sound, & controlled.
- Conclusions are well stated, linked to original research question & limited to supporting results.

Standout reviewing tips

The best reviewers use these techniques

Tip	***Example***
Support criticisms with evidence from the text or from other sources	*Smith et al (J of Methodology, 2005, V3, pp 123) have shown that the analysis you use in Lines 241-250 is not the most appropriate for this situation. Please explain why you used this method.*
Give specific suggestions on how to improve the manuscript	*Your introduction needs more detail. I suggest that you improve the description at lines 57- 86 to provide more justification for your study (specifically, you should expand upon the knowledge gap being filled).*
Comment on language and grammar issues	*The English language should be improved to ensure that an international audience can clearly understand your text. Some examples where the language could be improved include lines 23, 77, 121, 128 – the current phrasing makes comprehension difficult. I suggest you have a colleague who is proficient in English and familiar with the subject matter review your manuscript, or contact a professional editing service.*
Organize by importance of the issues, and number your points	*1. Your most important issue* *2. The next most important item* *3. …* *4. The least important points*
Please provide constructive criticism, and avoid personal opinions	*I thank you for providing the raw data, however your supplemental files need more descriptive metadata identifiers to be useful to future readers. Although your results are compelling, the data analysis should be improved in the following ways: AA, BB, CC*
Comment on strengths (as well as weaknesses) of the manuscript	*I commend the authors for their extensive data set, compiled over many years of detailed fieldwork. In addition, the manuscript is clearly written in professional, unambiguous language. If there is a weakness, it is in the statistical analysis (as I have noted above) which should be improved upon before Acceptance.*

Integrative taxonomy reveals three new species and one new record of *Psychropotes* (Holothuroidea, Elasipodida , Psychropotidae) from the Kermadec Trench region and the Wallaby-Zenith Fracture Zone

Yunlu Xiao [1, 2] , **Haibin Zhang** [Corresp. 1]

[1] Chinese Academy of Sciences, Institute of Deep-sea Science and Engineering, Sanya, Hainan, China
[2] University of Chinese Academy of Sciences, Beijing, China

Corresponding Author: Haibin Zhang
Email address: hzhang@idsse.ac.cn

The holothuroid genus *Psychropotes* is the largest genus in the family Psychropotidae. Prior to this study, this family contained 19 accepted species and was the dominant group in the deep-sea benthic fauna at lower bathyal-abyssal depths throughout the global oceans, but it has been poorly studied in the hadal zone. Deep-sea holothurians were collected in October 2022 to March 2023 by the joint China-New Zealand deep-diving scientific expedition to the Kermadec Trench in the South Pacific Ocean and the Wallaby-Zenith Fracture Zone in the East Indian Ocean at a depth of 6018–6605 m. Our examination of specimens of *Psychropotes* revealed three new species, which we described as *Psychropotes diutiuscauda* **sp. nov.**, *Psychropotes nigrimargaria* **sp. nov.**, and *Psychropotes asperatus* **sp. nov.** We also recorded *Psychropotes depressa* (Théel, 1882) for the first time from the Kermadec Arc at a depth of 1620 m. We provide comprehensive descriptions of the morphological features and a taxonomic key for the genus *Psychropotes*. We also performed a phylogenetic analysis of the order Elasipodida based on COI sequences and the concatenated 16S-COI sequences. Intraspecific and interspecific genetic distances were calculated among *Psychropotes* sp ecies based on COI sequences. Our phylogenetic analyses supported the assignment of three new species to the genus *Psychropotes* and their separation from congeners. The geographical distribution and global depth range of psychropotid species were summarized, and the results showed that the Pacific region had the highest species diversity. These findings contribute to the taxonomic diversity and patterns of geographical distribution in the family Psychropotidae.

Integrative taxonomy reveals three new species and one new record of *Psychropotes* (Holothuroidea, Elasipodida, Psychropotidae) from the Kermadec Trench region and the Wallaby-Zenith Fracture Zone

Yunlu Xiao[1,2] and Haibin Zhang[1]

1 Institute of Deep-sea Science and Engineering, Chinese Academy of Sciences, Sanya 572000, China

2 University of Chinese Academy of Sciences, Beijing 100049, China

Corresponding Author:

Haibin Zhang[1]

28 Luhuitou Road, Sanya, Hainan, 572000, China

E-mail address: hzhang@idsse.ac.cn

Abstract

The holothuroid genus *Psychropotes* is the largest genus in the family Psychropotidae. Prior to this study, this family contained 19 accepted species and was the dominant group in the deep-sea benthic fauna at lower bathyal-abyssal depths throughout the global oceans, but it has been poorly studied in the hadal zone. Deep-sea holothurians were collected in October 2022 to March 2023 by the joint China-New Zealand deep-diving scientific expedition to the Kermadec Trench in the South Pacific Ocean and the Wallaby-Zenith Fracture Zone in the East Indian Ocean at a depth of 6018–6605 m. Our examination of specimens of *Psychropotes* revealed three new species, which we described as *Psychropotes diutiuscauda* **sp. nov.**, *Psychropotes nigrimargaria* **sp. nov.**, and *Psychropotes asperatus* **sp. nov.** We also recorded *Psychropotes depressa* (Théel, 1882) for the first time from the Kermadec Arc at a depth of 1620 m. We provide comprehensive descriptions of the morphological features and a taxonomic key for the genus *Psychropotes*. We

also performed a phylogenetic analysis of the order Elasipodida based on COI sequences and the concatenated 16S-COI sequences. Intraspecific and interspecific genetic distances were calculated among *Psychropotes* species based on COI sequences. Our phylogenetic analyses supported the assignment of three new species to the genus *Psychropotes* and their separation from congeners. The geographical distribution and global depth range of psychropotid species were summarized, and the results showed that the Pacific region had the highest species diversity. These findings contribute to the taxonomic diversity and patterns of geographical distribution in the family Psychropotidae.

Keywords Deep-sea, Hadal zone, Morphology, New species, Phylogeny, Systematics

Introduction

Holothurians, also known as sea cucumbers, are the second most diverse class among echinoderms, with seven orders (*Miller et al., 2017*). They are primitive benthic animals distributed at all depths from shallow water to hadal zones (*Iken et al., 2001*; *Jamieson et al., 2011*; *Lee et al., 2017*), and they are abundant in many ecosystems, especially in the hadal zone (*Kuhnz et al., 2014*). Among the seven orders in the class Holothuroidea, the order Elasipodida Théel, 1882, which includes ~~the~~ families Psychropotidae Théel, 1882; Elpidiidae Théel, 1882; Laetmogonidae Ekman, 1926; and Pelagothuriidae Ludwig, 1893, is unique in being confined to the deep sea (*Hansen, 1975*). The family Psychropotidae includes 41 ~~accepted~~ species, which belong to three genera (*Psychropotes* Théel, 1882; *Benthodytes* Théel, 1882; and *Psycheotrephes* Théel, 1882). As the largest genus in Psychropotidae, *Psychropotes* contains 19 valid species (*WoRMS, 2024*): *Psychropotes belyaevi* Hansen, 1975; *P. depressa* (Théel, 1882); *P. dubiosa* Ludwig, 1893; *P. dyscrita* (Clark, 1920); *P. fuscopurpurea* Théel, 1882; *P. hyalinus* Pawson, 1985; *P. longicauda* Théel, 1882; *P. loveni* Théel, 1882; *P. minuta* Koehler & Vaney, 1905; *P. mirabilis* Hansen, 1975; *P. monstrosa* Théel, 1882; *P. moskalevi* Gebruk & Kremenetskaia in Gebruk et al., 2020; *P. pawsoni* Gebruk & Kremenetskaia in Gebruk et al., 2020; *P. raripes*

Ludwig, 1893; *P. scotiae* (Vaney, 1908); *P. semperiana* Théel, 1882; *P. verrucicaudatus* Xiao, Gong, Kou & Li, 2019; *P. verrucosa* (Ludwig, 1893); and *P. xenochromata* Rogacheva & Billett in Rogacheva et al., 2009. This genus was established by *Théel (1882)*, who erected four species discovered during the H.M.S Challenger Expedition. Species in *Psychropotes* are characterized by having a ventral anus, the presence of unpaired dorsal appendages, and the absence of circumoral papillae. As the distinctive members of deep-sea benthic communities at lower bathyal-abyssal depths throughout the world's oceans, this genus has revealed new species consistently in recent years (*Hansen, 1975*; *Rogacheva et al., 2009*; *Xiao, Li & Sha, 2018*; *Xiao et al., 2019*; *Gebruk, Kremenetskaia & Rouse, 2020*; *Yu et al., 2021*; *Yu et al., 2022*; *Xiao, Xiao & Zeng, 2023*; *Yuan, Wang & Zhang, 2024*). This genus has been found at hadal depths (6135–7250 m) across all non-polar oceans (*Ludwig,* 1893; *Hansen,* 1975; *Gebruk, Kremenetskaia & Rouse, 2020*).

The Kermadec Trench in the South Pacific Ocean is about 1195 km long and 120 km wide, with a maximum depth of ~10,106 m (*Jamieson et al.*, 2020; *Jamieson et al., 2024*). Holothurians are one of the most species-rich groups in the Kermadec Trench at hadal depths (*Jamieson et al.* 2020), but there are few reports and studies on deep-sea holothurians from the trench and its region. To date, *Benham (1912)* provided the only report of shallow holothuroid echinoderms for the Kermadec Islands. *Keable & Reid (2015)* reviewed the marine invertebrates collected during the Kermadec Biodiscovery Expedition 2011 and provided an inventory of invertebrates in the intertidal and subtidal habitats of the Kermadec Islands, which only included three shallow holothuroid species recorded by *O'Loughlin & Vandenspiegel (2012)*. Five species of *Psychropotes* have so far been reported from the South Pacific: *Psychropotes depressa*, *P. longicauda*, *P. loveni*, *P. monstrosa*, and *P. verrucosa*. Two of these were reported in the Kermadec Trench: *P. longicauda* and *P. loveni* (*Hansen, 1975*; *Gebruk, Kremenetskaia & Rouse, 2020*).

The Indian Ocean is the third largest ocean in the world, and it occupies nearly 20% of the global ocean volume, with an average depth of 3741 m (*Eakins & Sharman, 2010*). There are relatively few deep-sea biological studies in the Indian Ocean, and assessment of the deep-sea benthic fauna is rare from depths > 5000 m (*Parulekar et al., 1982*; *Janßen et al., 2000*; *Pavithran et al., 2009*; *Weston et al., 2021*). Compared with the central and western Indian Oceans, few studies have been conducted on benthic organisms at depths > 3000 m in the eastern Indian Ocean (*Post et al., 2021*; *Weston et al., 2021*; *Jamieson et al., 2022*), where studies have focused mainly on canyons, the Java Trench, and Wallaby-Zenith Fracture Zone (WZFZ). The WZFZ is located in the Wharton Basin of the East Indian Ocean, with complex geomorphological features and a maximum depth of 6625 m. In the survey of the WZFZ by Sonne in 2017, some species were reported for the first time in this area (*Weston et al., 2020*, *2021*), but the taxonomic studies of the WZFZ were very limited.

From October 2022 to March 2023, a joint China-New Zealand scientific expedition carried out a large-scale and systematic manned, deep-diving investigation and collected a number of holothurian specimens (*Peng et al., 2023*). Based on morphological and molecular phylogenetic analyses, three new species (i.e., *Psychropotes asperatus* sp. nov., *Psychropotes diutiuscauda* sp. nov., and *Psychropotes nigrimargaria* sp. nov.) and one new record (i.e., *Psychropotes depressa*) of the genus *Psychropotes* were discovered. We provide detailed descriptions of ~~three new species, one new record,~~ and a taxonomic key for the genus *Psychropotes.* We analyzed their phylogenetic relationships within elasipodid species and the inter- and intraspecific divergence among nine species of *Psychropotes*. In addition, we also discuss the diversity and distribution of psychropotid holothurians.

Materials & Methods

Sampling and preservation

The human-occupied vehicle (HOV) 'Fendouzhe' was used to collect *Psychropotes* specimens from the Kermadec Trench region in the South Pacific and the WZFZ in the East Indian Ocean (October 2022–March 2023) (Fig. 1). Specimens were sampled and photographed *in situ* using HOV cameras. For morphological analyses, specimens were photographed promptly after collection and then fixed in 99% high grade absolute ethanol. Two specimens (i.e., FDZ188-F01 & FDZ188-F02) collected from WZFZ were deposited in the Institute of Deep-sea Science and Engineering (IDSSE), Chinese Academy of Sciences (CAS), Sanya, China. The other two specimens (i.e., NIWA164003 & NIWA164160) that were collected from Kermadec Trench were registered onboard using the Specify *niwainvert* database of National Institute of Water and Atmospheric Research (NIWA) and were loaned by the NIWA Invertebrate Collection (NIC) to IDSSE.

Morphological observations

General morphology was studied by means of a dissecting stereomicroscope (OLYMPUS SZX7). Ossicles were obtained from the dorsal and ventral body walls, tentacles, dorsal papillae, and tube feet by digestion of tissues in a solution of 15% sodium hypochlorite, and then they were washed with distilled water and 75% ethanol. To investigate the ultrastructure of ossicles, ossicles were air-dried, coated with gold, and observed using a scanning electron microscope (SEM). SEM imaging was performed using a Phenom ProX scanning electron microscope. For the identity and terminology of the ossicles, we followed *Hansen (1975)* and *Gebruk, Kremenetskaia & Rouse (2020)*.

DNA extraction and sequencing

Total genomic DNA was extracted from small pieces of 20–30 mg holothurian muscle tissue of each specimen using a TIANamp Marine Animals DNA Kit (TianGen, Beijing), following the manufacturer's instructions. The PCR amplification for 5'-end of mitochondrial cytochrome c oxidase I (COI) and 16S rRNA were conducted using the primers that were outlined in *Miller et al. (2017)* as follows: initial denaturation at 98 °C for 3 min, followed by 40 cycles at 98 °C for 10 s, 52 °C for 10s, 72 °C for 10s, and a final extension at 72 °C for 5 min. The total reaction volume was 50 µL that included 2 µL of template DNA, 1 µL of each primer, and 46 µL of GoldenStar® T6Super PCR Mix (1.1×). PCR products were assessed on GelRed-stained 1.5%

agarose gel electrophoresis and sequenced in both directions using the ABI 3730 DNA Analyzer sequencing facility from BGI Genomics, Shenzhen, Guangdong Province, China. The final sequences were deposited in the Science Data Bank of Chinese Academy of Sciences (*Xiao & Zhang, 2024*) and the GenBank database with the accession numbers PP869369–PP869372 (COI) and PP868346–PP868349 (16S).

Phylogenetic analyses and genetic distance

Molecular phylogenetic analyses were conducted using two partial sequences (COI and 16S) obtained from each of the four specimens in this study and some relevant sequences of elasipodid species and the out-group species of the genus *Pseudostichopus* Théel, 1886 (Holothuroidea, Persiculida, Pseudostichopodidae), which was downloaded from National Center for Biotechnology Information (NCBI). A final total of 54 16S sequences and 54 COI sequences were obtained (Appendix 1). For the phylogenetic investigation, we created the alignment datasets of the COI and the concatenated regions of 16S and COI (16S-COI). The sequences were aligned using MAFFT v.7 (*Katoh & Standley, 2013*) with default parameters. The evolutionary model GTR + G+ I was the best-fitted model for both alignments, which was selected using PartitionFinder2 (*Lanfear et al., 2017*), with all algorithms and AICc criteria. Maximum Likelihood (ML) analysis was inferred using the Shimodaira-Hasegawa-like approximation, likelihood-ratio test (*Gascuel, 2010*) and IQ-TREE (*Lam-Tung et al., 2015*) models with 20,000 ultrafast bootstraps (*Minh et al., 2013*). For the ML bootstraps, we considered values $< 70\%$ as low, 70–94% as moderate, and $\geq 95\%$ as high, following *Hillis & Bull (1993)*. Bayesian Inference phylogenies (BI) were inferred using MrBayes 3.2.6 (*Ronquist et al., 2012*) under the partition model (two parallel runs, 5,000,000 generations). The initial 25% of sampled data were discarded as burn-in, and the remaining trees were summarized in a 50% majority rule consensus tree. For the Bayesian posterior probabilities, we considered values < 0.95 as low and > 0.95 as high, following *Alfaro et al. (2003)*. The results were visualized using FigTree v. 1.4.4 (*Rambaut, 2018*). We estimated the genetic distances of COI, which were calculated using the Kimura two-parameter model, within each *Psychropotes* species and among different *Psychropotes* species using model MEGA X (*Kumar et al., 2018*).

Analyses of species diversity and distribution

Existing distribution data of psychropotid species were extracted from the Ocean Biodiversity Information System (OBIS) (https://obis.org/) and the Global Biodiversity Information Facility (GBIF) (https://www.gbif.org/zh/), from published literature, and from this study. The distribution of three genera in the family Psychropotidae was illustrated using Generic Mapping Tools, which is a cartographic scripting toolset developed by *Wessel & Smith (1995)*. Using the World Register of Marine Species (WoRMS) and primary literature (e.g. *Vaney, 1908*; *Théel, 1882*; *Ludwig, 1893*; *Koehler & Vaney, 1905*; *Hansen, 1975*; *Gebruk, 2008*; *Rogacheva et al., 2009*; *Li et al., 2018*; *Xiao, Li & Sha, 2018*; *Gebruk, Kremenetskaia & Rouse, 2020*), we obtained all ~~accepted~~ species in the family and discussed the geographical distribution of different groups.

Results

Systematics

Order Elasipodida Théel, 1882

Family Psychropotidae Théel, 1882

Genus *Psychropotes* Théel, 1882

***Psychropotes asperatus* sp. nov.**

(Figs. 2–4)

urn:lsid:zoobank.org:act:FF8C7F3A-D0AA-44D3-9C83-7A9D4032D0A2

Material examined. Holotype. NIWA164003, collected from the overriding plate of Kermadec Trench in the South Pacific Ocean, Dive FDZ126 (30°25.51′S, 177°54.60′W), depth 6018 m, 1

Nov. 2022, preserved in 99% high grade absolute ethanol.

Type locality. The Kermadec Trench, South Pacific Ocean, depth 6018 m.

Diagnosis. Body elongated, dorsum convex, ventrum flattened. Brim narrow. Mouth ventral, anus ventral. Tentacles 12. Dorsal papillae not found. Unpaired appendage about $^{1}/_{3}$ of body length, end bifurcated, placed about $^{1}/_{3}$ of body length from posterior body end. Color violet, dorsal skin and unpaired appendage covered with warts. Dorsal deposits two types, large crosses and small deposits with three, four, and five arms. Unpaired dorsal appendage with large crosses. Tentacles and tube feet with rods. Ventral deposits small crosses, rods, and tripartite deposits.

Description. External morphology. Body elongated, dorsum convex, ventrum flattened (Figs. 2A and 2B). 15 cm long and 7.5 cm wide after fixation (Figs. 2C–2D). Color in life violet, darker in the middle of the dorsum and ventrum. Dorsal skin gelatinous and soft, with a rough surface and conspicuous warts (Figs. 2C, 2E and 2F), ventral skin smooth (Fig. 2D). Mouth ventral, anus ventral. Tentacle 12, completely retracted into pockets of the skin, with round terminal discs, circum-oral papillae absent. Brim fused with tube feet, relatively narrow, retracted when fixed (Figs. 2C and 2D). Midventral tube feet small, arranged along the middle of ventrum. Dorsal papillae not found. The unpaired dorsal appendage end bifurcated (Figs. 2A and 2B) *in situ*. In preserved state, unpaired dorsal appendage 4.6 cm long, about $^{1}/_{3}$ of body length, 2.5 cm at the base, placed about $^{1}/_{3}$ of body length from the posterior end (Fig. 2C), covered with warts as on the dorsal surface of the body.

Ossicle morphology. Dorsal deposits with two main types. (1) Large crosses (Figs. 3A–3E) with arms 375–620 µm in length, bent downwards or irregular bending direction (Fig. 3C), bearing small spines; central apophysis long, spinose (Figs. 3A–3D) or smooth (Fig. 3E), 188–375 µm in length. (2) Small deposits with three, four, and five arms almost straight, central apophysis short or rudimentary (Fig. 3F). Deposits with four arms slender, varying in length from short to long (57–207 µm in length), with sparse or conspicuous spines (sometimes bifurcated); tripartite deposits with conspicuous spines, proximal spines often bifurcated, three arms almost equal in length, each arm about 162 µm long, central apophysis short or reduced;

quinquepartite deposits, five arms almost equal in length, each arm 80 µm long, central apophysis branched or rudimentary. Crosses and rods found in unpaired dorsal appendage (Figs. 3G–3L). Crosses with single central apophysis, 147–213 µm in length, bearing spines (Figs. 3H, 3I, 3K and 3L) or smooth (Fig. 3G), arms bent downwards from central apophysis, 238–500 µm in length, sometimes with irregular curvature; rods up to 427 µm long (Fig. 3J), with the branch emanating from the center forming a 'third arm', only the ends possessing spines. Tentacles with three types of rods (Figs. 4A–4D). (1) Sturdy and rather large rods (Figs. 4A and 4C), up to 1.3 mm long, terminal part rounded, bearing spines. (2) Tripartite deposits (Fig. 4B), each arm about 505 µm long. (3) Smooth rods (Fig. 4D), 333 µm in length. Deposits of tube feet rods (Figs. 4E and 4F), up to 639 µm in length, ends bearing small spines. Simple rods, tripartite deposits and crosses in ventral body wall (Figs. 4G–4J), rods (Fig. 4I) same as those in tube feet, tripartite deposits (Fig. 4J) similar to those in tentacles, but smaller, each arm about 160 µm in length, arms of smaller crosses 92–150 µm in length, with spines distributed over at least distal half, central apophysis rudimentary (Figs. 4G and 4H).

Etymology. The species name is derived from the Latin word *asperatus*, which means rough, and this refers to the rough dorsal skin caused by warts.

Distribution. Only known in the type locality.

Remarks. *Psychropotes asperatus* sp. nov. clearly belongs to the genus *Psychropotes*, and it differs from other congeners by the tripartite and quinquepartite deposits on the dorsum and from the rather robust and large rods in tentacles.

The dorsal body wall and unpaired appendages of the new species were covered with warts; this made it most similar to *P. verrucicaudatus*, which was described by *Xiao et al. (2019)* based on one specimen collected from the South China Sea. Morphologically, the new species differed from *P. verrucicaudatus* by the length and position of the dorsal appendage, and there were some differences in ossicle characters. In *P. verrucicaudatus*, the appendage was very short, measured about $^{1}/_{12}$ of the body length, placed about $^{2}/_{5}$ of the body length from the posterior end of the body, but in the new species, the appendage was about $^{1}/_{3}$ of the body length, and it was placed about $^{1}/_{3}$ of the body length from the posterior end of the body. In ossicle morphology, *Psychropotes asperatus* sp. nov. had large crosses with arms of 375–620 µm, but these were smaller than the giant crosses of *P. verrucicaudatus*, which had arms 600–750 µm in length. In addition, in *P. verrucicaudatus*, the central apophysis of giant crosses bear spines, but in the new species, the crosses had a central apophysis that was spinous or smooth. The new species was differentiated from *P. verrucicaudatus* by possessing tripartite and quinquepartite deposits on the dorsum in addition to crosses. For the rods in the tentacles, those of *P. verrucicaudatus* were 210–600 µm long with multiple and irregularly arranged spines, whereas the rods of the new species were more robust, up to 1.3 mm long, and with spines only at the ends.

***Psychropotes diutiuscauda* sp. nov.**

(Figs. 5–8)

urn:lsid:zoobank.org:act:E7FE330B-DA67-4D70-B1F6-6CA468E47874

Materials examined. Holotype. FDZ188-F01, collected from the WZFZ in the East Indian Ocean, Dive FDZ188 (22°23' S, 102°27' E), depth 6397 m, 25 Feb. 2023, preserved in 99% high grade absolute ethanol.

Type locality. WZFZ, East Indian Ocean, depth 6397 m.

Diagnosis. Body elongated, color yellowish green. Tentacles 15. Brim broad on anterior end of the body. Ventrolateral tube feet up to nine pairs. Midventral tube feet small, arranged in two rows. Unpaired appendage rather large, about 1.5 times as long as body length, placed close to posterior end of the body. Dorsal deposits cross-shaped, quinquepartite. Tentacles with rather large rods and smaller crosses. Tube feet crosses with single and two central apophysis, short or longer than the arms. Ventral deposits irregular rods, crosses, and quinquepartite deposits, single or two central apophysis on under side of the crosses.

Description. External morphology. Body elongated, convex dorsally and flattened ventrally (Figs. 5A–5C), about 17 cm long and 7 cm wide *in situ*, 9 cm in maximum width in the anterior apart *in situ*. Unpaired dorsal appendage rather large, 24 cm long *in situ*, 1.5 times the length of the body (Figs. 5A–5C), place close to posterior end of the body. In preserved state, body 9 cm in length and 4 cm in width (Figs. 5D and 5E), unpaired dorsal appendage rather large and long, 11.5 cm in length, and as rough as the dorsal skin. Color yellowish green (Figs. 5A–5E), skin rough. Tentacles 15, shield-shaped. Brim well developed at anterior end of the body (Fig. 5A). Ventrolateral tube feet approximately nine pairs, arranged along the entire edge of the brim. Dorsal papillae not found. Midventral tube feet small, present throughout the whole length of the ventral sole.

Ossicle morphology. Dorsal deposits crosses and quinquepartite. (1) Arms of crosses, usually with a horizontal curvature (Figs. 6E–6I), 90–210 μm in length. The spines numerous and large, tapering toward the end of the arms, with irregular or secondary spines, central apophysis replaced by branched spines. (2) Quinquepartite deposits (Fig. 6D), each arm 140–230 μm in length, bearing irregular spines, proximal spines larger than others, bifurcate or tripartite, central apophysis replaced by multiple spines. (3) Irregular crosses with extremely slender arms (Figs. 6A–6C), 70–160 μm in length, small unbranched spines alternately spaced above and below on arms. Deposits on ventrum crosses and quinquepartite (Figs. 7A–7P). Quinquepartite deposits with single central apophysis or reduced, each arm 40–90 μm in length (Figs. 7A–7C), bearing spines. Crosses of two types: (1) Arms varing from almost straight to sharply bent (Figs. 7D–7N), 30–90 μm in length, with prominent irregular spines. Four types of central apophysis: single (Figs. 7D–7I), reduced (Figs. 7J, 7K), two central apophysis (Figs. 7L and 7M) on under side of the crosses, or tripartite (Fig. 7N), 10–20 μm in length, bearing branched spines. (2) Relatively slender crosses (Figs. 7O and 7P), arms 40–140 μm in length, at least half of the arms with small spines, single central apophysis spinous. Deposits on tube feet with three types of crosses (Figs. 8A–8Q). (1) Crosses with arms 80–220 μm in length, densely distributed with conspicuous spines, proximal spines larger than others, often bifurcate or tripartite, sometimes bearing irregular secondary spines. Single central apophysis relatively short, equal in length to proximal large spines (Figs. 8A–8D), or rather long, almost equal to the length of the arms (Figs.

8G–8I), 130–280 µm long, forming a "fifth arm", apophysis also spinous. (2) Crosses with two short or two long central apophysis (Figs. 8J and 8K), bearing spines. (3) Crosses with slender arms (Figs. 8M–8Q), 160–190 µm in length, central apophysis often reduced. Rather large rods and smaller crosses in tentacles (Figs. 8R–8V), rods up to 1 mm long, some with an extra branch from the center (Figs. 8R and 8V), bearing irregular small spines; crosses with spinose arms 40–90 µm in length (Fig. 8V), conspicuous spines distributed over at least distal half, central apophysis rudimentary.

Etymology. From Latin '*diutius*' for longer, and '*cauda*', meaning tail. The name refers to its dorsal appendage that was longer than its body length.

Distribution. Only known in the type locality.

Remarks. The new species clearly belongs to *Psychropotes*, the unpaired dorsal appendages of '*Psychropotes longicauda*' species were usually $^{1}/_{5}$–$^{1}/_{1}$ length of the body, whereas the appendages of the new species were about 1.5 times the length of the body. *Psychropotes diutiuscauda* sp. nov. differed from other species of *Psychropotes* by the presence of quinquepartite deposits on the dorsum and ventrum, and ventral crosses were strongly spinous, with reduced, tripartite, single or two central apophyses developed on the underside of the crosses.

The unique yellowish-green color made *Psychropotes diutiuscauda* sp. nov. most similar to *P. xenochromata*, *P. dyscrita*, and *P. moskalevi*. Compared with the 18 tentacles of the other three species, the number of tentacles of the new species was fewer, only 15. The length of unpaired dorsal appendage was 1.5 times of the body length in the new species, but the unpaired dorsal appendages were $^{1}/_{5}$–$^{1}/_{2}$ of the body length in *P. xenochoromata*, $^{1}/_{5}$–$^{1}/_{1}$ of the body length in *P. moskalevi*, and $^{4}/_{5}$ of the body length in *P. dyscrita*. Among the yellowish-green species, *Psychropotes diutiuscauda* sp. nov. matched well with *P. moskalevi* with its dorsal deposits of horizontally curved arms, short spines on the arms, with proximal spines often bipartite or bearing secondary spines, which were about the same length as the central apophysis. However, the new species differed from *P. moskalevi* by possessing quinquepartite deposits on the dorsum and ventrum, by the absence of tripartite spines? and rods on the ventrum, and by ventral crosses that were strongly spinous, with single, reduced, and two central apophyses, which were developed on the underside of the crosses.

***Psychropotes nigrimargaria* sp. nov.**

(Figs. 9–11)

urn:lsid:zoobank.org:act:2C252D0F-16BA-4E6E-9F17-D8AF01D43CB8

Materials examined. Holotype. FDZ188-F02, collected from the WZFZ in the East Indian Ocean, Dive FDZ188 (22°22' S, 102°27' E), depth 6605 m, 25 Feb. 2023, preserved in 99% high grade absolute ethanol.

Type locality. WZFZ, East Indian Ocean, depth 6605 m.

Diagnosis. Body elongated, up to 30 cm long. Color dark violet, tentacles, and tube feet darker. Tentacles 18, with round terminal discs. Brim broad, especially at anterior and posterior ends. Free ventrolateral tube feet 12 pairs. Unpaired dorsal appendage about $^{1}/_{3}$ of body length placed some distance from the posterior end. Dorsal deposit crosses, central apophysis tripartite or quadripartite. Crosses and rods in tentacles. Tube feet deposits crosses, tripartite, and rods. Ventral crosses smaller than the dorsal ones.

Description. External morphology. Body elongated, about 30 cm long and 10 cm wide *in situ* (Figs. 9A and 9B). In preserved state, body approximately 16.5 cm in length and 8 cm in width (Figs. 9D and 9E). Color dark violet, tentacles, and tube feet darker, almost black. Skin thick. Tentacles 18, with round terminal discs (Figs. 9C and 9E). Brim well developed especially at anterior and posterior ends of the body, with maximum width around anterior end of 11 cm (Figs. 9A and 9B). Free ventrolateral tube feet 12 pairs, retracted into the body after fixation. The mid-ventral tube feet in poor condition, and not clearly observed. Dorsal papillae not found. Unpaired dorsal appendage conspicuous and conical, tapering toward the end, *in situ* 10 cm long, about $^{1}/_{3}$ of the body length (Figs. 9A and 9B); in preserved state, 6 cm long, developed at 3 cm from posterior body end (Figs. 9D and 9E).

Ossicle morphology. Dorsal deposits crosses with arms 80–310 μm in length (Figs. 10A–10G), sharply bent downwards, arm spines conspicuous; bearing 1–3 proximal spines, the largest spines often bipartite or irregular branched, their length equal to that of central apophysis, additional smaller spines on arm ends. Central apophysis tripartite or quadripartite (Figs. 10D–10G). Ventral crosses smaller than the dorsal ones, with arms 40–120 μm in length, bearing fewer spines, and central apophysis reduced or short (Figs. 10H–10J). Tube feet crosses, tripartite deposits, and rods (Figs. 11A–11K), crosses with arms 90–190 μm long, similar to dorsal crosses (Figs. 11A–11C and 11E–11G) and ventral crosses (Figs. 11I–11K) but smaller; robust rods up to 400 μm long (Fig. 11H); tripartite deposits with spines at the ends (Fig. 11D and 11H). Crosses and rods in tentacles (Figs. 11L–11N), crosses with arms 80–160 μm in length, bearing small spines or smooth, irregularly spinous central apophysis short or reduced (Fig. 11L); rods up to 540 μm in length, smooth or spinous ends branched (Figs. 11M and 11N), some possessing an extra branch in the middle (Fig. 11M).

Etymology. From Latin, *nigri*, black, and *margaria*, pearl, meaning “black pearl”, which alludes to the shape and color of the tentacles of this species.

Distribution. Only known in the type locality.

Remarks. Arms of dorsal crosses bear large proximal spines, bipartite or branched irregularly, and the length of proximal spines were equal to that of the central apophysis, which made the new species most similar to *P. raripes* and *P. monstrosa*.

However, *Psychropotes nigrimargaria* sp. nov. differed from *P. raripes* by the absence of dorsal papillae, *P. raripes* has 5–7 pairs. The number of free ventrolateral tube feet in *P. raripes* was 7–10 pairs, but the new species had 12 pairs. Unpaired dorsal appendages were up to $^{3}/_{4}$ of the body length in *P. raripes* and placed close to the posterior end of the body, but in the new species they were about $^{1}/_{3}$ of the body length and developed at ~$^{1}/_{5}$ of the body length from posterior end. For ossicle morphology, *Psychropotes nigrimargaria* sp. nov. had dorsal crosses with central apophyses that were tripartite and quadripartite and ventral small crosses with fewer spines on the arms, while *P. raripes* had dorsal crosses with central apophyses that were tripartite, tripartite deposits; ventral crosses tripartite, and star-shaped deposits with conspicuous spines on the arms.

Psychropotes nigrimargaria sp. nov. differed from *P. monstrosa* by the absence of dorsal papillae, *P. monstrosa* had 5–7 pairs. The number of free ventrolateral tube feet in *P. monstrosa* was 18–20 pairs, but the new species had 12 pairs. The unpaired dorsal appendage was almost $^{1}/_{2}$ of the body length in *P. monstrosa*, and it was about $^{1}/_{3}$ of the body length in the new species. For ossicle morphology, the new species differed from *P. monstrosa* by the absence of dorsal deposits with strongly arcuate arms, and the presence of tripartite and quadripartite central apophyses that were unbranched in *P. monstrosa.*

***Psychropotes depressa* (Théel, 1882)**

(Figs. 12 and 13)

Euphronides depressa Théel, 1882, pp. 93–96, pl. XXVI, XXXV, XL, XLVI; *Ohshima, 1915*, pp. 244–245, fig.1.

Psychropotes depressa Hansen, 1975, pp. 106–111, fig. 43, 44, pl. VII, XII, XIV; *Gebruk, 2008*, pp. 50–51; *Rogacheva et al., 2013*, pp. 599, fig. 17f,g; ~~*Xiao*~~ *Xiao, Li & Sha, 2018*, pp. 5–10, fig. 6–10.

Euphronides depressa var. minor *Théel, 1886*, p. 2.

Euphronides cornuta Verrill, 1884, p. 217; *Veriill, 1885*, pp. 518, 538, fig. 32, 33; *Deichmann, 1930*, pp. 127–128; *Heding, 1940*, p. 368.

Euphronides tanneri Ludwig, 1894, pp. 39–44, pl. III, IV, V.

Euphronides auriculata Perrier, 1896, pp. 901–902; *Perrier, 1902*, pp. 434–438, pl. XIII, XX; *Grieg, 1921*, pp. 8, 9.

Euphronides violacea Perrier, 1896, p. 902; *Perrier, 1902*: 438–441, plate XX; *Deichmann, 1930*, pp. 128–129; *Deichmann, 1940*, pp. 201–202; *Heding, 1942*, pp. 15–16; *Madsen, 1947*, p.

16; *Deichmann, 1954*, p. 384.

Euphronides talismani Perrier, 1896, p. 902; *Perrier, 1902*, pp. 441–444, plate XX; *Hérouard, 1902*, pp. 30–31, plate II; *Deichmann, 1930*, p. 129; *Heding, 1942*, p. 15, fig. 15.

Benthodytes assimilis Théel, 1886, pp. 2–3.

Material examined. NIWA164160, collected from the Kermadec Arc in the South Pacific Ocean, Dive FDZ150 (27°34.54'S, 177°8.51'W), depth 1620 m, 8 Dec. 2022, preserved in 99% high grade absolute ethanol.

Description. External morphology. The specimen 27 cm long and 9.5 cm wide *in situ* (Fig. 12A), color violet, slightly darker on ventrum (Fig. 12B). After several days of fixation in 99% high grade absolute ethanol, body flattened, 9 cm long and 4 cm maximum width in anterior part (Fig. 12B). Tentacle 12, round terminal discs with short, digitiform projections on the margin. Brim broad. Midventral tube feet small, arranged in two rows. Dorsal papillae five pairs (Figs. 12A and 12B), minute, gradually increasing the interval and number; the fifth pair of papillae largest, 9 mm in length, and placed about $^{1}/_{2}$ of the body from posterior end. In preserved state (Fig. 12B), unpaired appendage 2.2 cm long, and 2 cm wide at the base, placed in 2.7 cm (about $^{1}/_{3}$ of body length) from the posterior end.

Ossicle morphology. Dorsal crosses with slender arms (Figs. 12C–12J and 13B), long and smooth central apophysis, arms 144–349 μm in length, bent downwards proximally, and slightly curved upwards or horizontal in the distal part. Arms often with four proximal spines, about $^{3}/_{5}$ of the length of the central apophysis (Figs. 12C, 12D, 12G and 12I), or shorter than central apophysis but larger than other spines (Figs. 12E and 12J). After repeated examinations, ventral deposits not found. Dorsal papillae crosses (Fig. 13A), arms up to 270 μm in length, sharply curved downward and then upward at the end, bearing smaller proximal spines. Deposits of the unpaired appendage similar to those on dorsum (Fig. 13C). Tentacles with simple rods (Fig. 13D), 255–353 μm in length.

Distribution. This species is common throughout the North Atlantic and South Atlantic, and

Pacific Ocean (Japan, Caroline seamount, Gulf of Panama, Chile, and the Kermadec Arc). Depth 957–4200 m.

Remarks. This species has a wide geographical distribution and exhibited a high degree of variability in its morphological characteristics *(Hansen 1975*; *Xiao, Li & Sha, 2018)*. There have been several synonyms (*Théel, 1882*; *Verrill, 1884*; *Théel, 1886*; *Perrier, 1896*; *Hérouard, 1902*; *Perrier, 1902*; *Deichmann, 1930*), and the synonymous species were distinguished from each other by the shape of the body, the size of the posterior-most pair of dorsal papillae, the size of the unpaired appendage, body color, and the size and shape of deposits. By re-examining the specimen and comparing descriptions in the literature, *Hansen (1975)* determined that none of these differences were valid identifying characters and that there were age variations in some features, such as the number of tentacles, skin texture, the size of the posterior-most pair of dorsal papillae; geographic variation may cause changes in certain features, such as the shape and size of crosses and whether or not the long central apophysis bear spines.

The morphological features of the specimen in this study, which included the position and length of the unpaired dorsal appendage and the types of ossicles, were consistent with those of *P. depressa*. However, the following differences in morphological features occurred: (1) five pairs of dorsal papillae, (2) deposits not found on ventrum, (3) the posterior-most pair of papillae were larger than the others, and (4) only 12 tentacles instead of the usual 18 tentacles. Our specimen conformed to the known range of variation in *P. depressa* that was described by *Hansen (1975)*, *Ohshima (1915)*, and *Xiao, Li & Sha (2018)*. Therefore, we identified it as *P. depressa*. This was the first record of *P. depressa* from the Kermadec Trench. In addition, we supplemented a description of the dorsal papillae deposits (Fig. 6A), which were more similar to the original description of the dorsal surfaced crosses, but this trait was not mentioned in the original literature. The arms were bent sharply downward, then upward at the ends, and arms bear smaller spines near the central apophysis.

Key to the species of *Psychropotes* Théel, 1882 (revised from *Xiao et al. 2019*)

1. Body transparent, colorless ··································· *P. hyalinus*

Body non-transparent, colored ··································· 2

2. Body yellowish or yellow-greenish ··································· 3

Body violet or purple ··································· 6

3. Tentacles 17–20, the appendage is $^{1}/_{5}$–$^{1}/_{1}$ of body length ··································· 4

Tentacles 15, the appendage is 1.5 times of body length ····· *P. diutiuscauda* sp. nov.

4. With free ventrolateral tube feet ··································· 5

Without free ventrolateral tube feet ··································· *P. xenochromata*

5. Ventrolateral tube feet 13–15 pairs, dorsal papillae absent ······················ *P. dyscrita*

Ventrolateral tube feet up to 25 (often 17–19) pairs, dorsal papillae up to 8 pairs ···· ··································· *P. moskalevi*

6. Dorsal appendage placed close to posterior end of body ··································· 7

Dorsal appendage placed at least $^{1}/_{5}$ body length from posterior end of body ······· 12

7. Tentacles 10-12 ··································· 8

Tentacles 18 ··································· 9

8. Ventral crosses with a low and spinous central apophysis, or with no apophysis, arms up to 0.2 mm long, with small spines ··································· *P. loveni*

Ventral crosses with long arms (up to 0.3 mm) and long central apophysis, without spines ··································· *P. dubiosa*

9. Dorsal papillae present ··································· 10

Dorsal papillae absent ··································· *P. nigrimargaria* sp. nov.

10. Relatively a low number of ventrolateral tube feet, 7-10 pairs ················ *P. raripes*

Relatively a high number of ventrolateral tube feet, up to 26 pairs ····················· 11

11. Dorsal ossicles with arms only of short type, 0.06–0.1 mm in length; dorsal papillae small, 4 pairs ··································· *P. fuscopurpurea*

Dorsal ossicles with arms of both short and long types, 0.06 mm or 0.24-0.4 mm in length; dorsal papillae minute, 5 pairs ··································· *P. longicauda*

12. Dorsal skin covered with warts ··········· 13

Dorsal skin smooth ··········· 14

13. Dorsal appendage covered with warts ··········· 15

Dorsal appendage smooth ··········· 16

14. Dorsal appendage at the most $^{1}/_{6}$ length of the body ··········· 17

Dorsal appendage at least ⅓ length of the body ··········· 18

15. The appendage is very short, measured about $^{1}/_{12}$ of body length, placed about $^{2}/_{5}$ of body length from posterior end of body ··········· *P. verrucicaudatus*

The appendage is $^{1}/_{3}$ of body length and placed about $^{1}/_{3}$ of body length from post-erior end of body ··········· *P. asperatus* sp. nov.

16. Dorsal appendage short ··········· *P. verrucosa*

Dorsal appendage very long ··········· *P. mirabilis*

17. Tentacles 18 ··········· *P. depressa*

Tentacles 16 ··········· *P. scotiae*

18. Brim broad. Dorsal appendage ⅓ to $^{1}/_{2}$. length of the body ··········· 19

Brim narrow. Dorsal appendage ⅓ to $^{1}/_{1}$ length of the body ··········· 20

19. Dorsal papillae up to 3 pairs, dorsal crosses with small spines placed in rings on the arms, central apophysis rudimentary or absent ··········· *P. belyaevi*

Dorsal papillae 5–7 pairs, dorsal crosses with strongly bent arms, bearing two proximal spines, central apophysis large ··········· *P. monstrosa*

20. Tentacles 15–16, without free ventrolateral tube feet ··········· 21

Tentacles 18, free ventrolateral feet 20–21 pairs ··········· *P. pawsoni*

21. Two types of ossicles: one with spines throughout arm length, the other with a smooth, proximal arm part and a high, central apophysis ending in three or four downwardly bent hooks ··········· *P. semperiana*

Only one type of ossicles: small, slender crosses with a low, central apophysis ··········· *P. minuta*

Genetic distances and phylogenetic analyses

A total of four COI sequences and four 16S sequences from three new species and one new record were deposited into GenBank (Appendix 1). The COI sequences from nine species of *Psychropotes* were used to perform pairwise, uncorrected p-distance analyses based on the Kimura two-parameter (K2P) model (Table 1). For COI alignment, the interspecific distances ranged between 1.38–13.54%, and the intraspecific distances ranged from 0.00 to 1.23% (Table 1).

We conducted the molecular phylogenetic analysis of the order Elasipodida based on all available sequences of four families, and their sampling information and accession numbers are provided in Appendix 1. Finally, 640 bp partial COI and 516 bp partial 16S sequences were obtained after removing non-homologous sites from the sequence alignments, and these were used to reconstruct the BI and ML trees. Compared with phylogenetic trees based on concatenated 16S-COI sequences of length 1157 bp, those trees that were based solely on the 640 bp mitochondrial COI gene provided a higher resolution and nodal support (Figs. 14 and 15).

The four families were grouped together and formed a clade in our phylogenetic analyses, and the topological structures of the ML and BI trees were consistent with the traditional classification system. Tree topologies showed that Elpidiidae, Pelagothuriidae, and Psychropotidae were monophyletic, and Laetmogonidae was polyphyletic. For Laetmogonidae, the molecular evidence was inconsistent with the morphological taxonomy, moreover, the phylogenetic trees based on concatenated 16-COI loci and a single COI locus showed somewhat different topological structures. In the 16S-COI trees (Fig. 15), the phylogenetic relationships of the family Laetmogonidae were clustered into two portions. Portion 1: Species of *Laetmogone* formed a single clade (ML 100, BI 1). Portion 2: Species in genera *Pannychia*, *Benthogone*, and *Psychronaetes* were grouped with low support (ML 72, BI 0.94). The only species in the family Pelagothuriidae, *Enypniastes eximia* Théel, 1882, clustered with *Psychronaetes* isolates (ML 68, BI 0.75), and it nested within Laetmogonidae. In the COI trees (Fig. 14), species of *Laetmogone* formed a single clade (ML 100, BI 1), but the remaining three genera were not clustered together, each branch had very low support (Fig. 14), and *Enypniastes eximia* formed a single clade with low support (ML 71). The results showed poor support, which was likely due to the limited sequences available for Laetmogonidae and Pelagothuriidae, therefore, more molecular data need to be obtained for further study.

For Elpidiidae, the phylogenetic reconstructions of single COI loci showed quite similar topologies compared with concatenated 16S-COI trees, and they provided higher resolution (Figs. 14 and 15). Hence, we only used the topologies of the COI trees for checking the phylogenetic relationships of Elpidiidae (Fig. 14). Species in *Peniagone* were grouped with a single clade (ML 100, BI 1), sister to clade *Amperima* + *Protelpidia* + *Scotoplanes* + *Elpidia* (ML 97, BI 1). The monophyly of the genera *Peniagone* and *Elpidia* were well supported (ML 100, BI 1). For the other three genera, the monophyly of *Amperima*, *Protelpidia*, and *Scotoplanes* could not be verified because we had molecular data for only one species in each genus.

In Psychropotidae, the phylogenetic analyses based on the combined genes (16S-COI) and the single COI gene were similar, except for *P. longicauda* and *P.* cf. *semperiana* in 16S-COI trees (the two species were absent in the COI trees). The COI trees provided higher quality support, thus, the topologies of these reconstructed trees based on a single COI gene were described here. *Benthodytes* was paraphyletic and divided into two clades with high support (Clade I: ML 95, BI 0.97; Clade II: ML 100, BI 1), which was inconsistent with the traditional classification system. The three new species and one new record from the Kermadec Trench fell into the genus *Psychropotes*, which was a monophyletic group (ML 98, BI 0.99). *Psychropotes* had three ~~clades. Clade~~ 1: *Psychropotes depressa* independently formed a sister clade with all other congeners in *Psychropotes* (ML 98, BI 0.99); ~~clade~~ 2: *P. diutiuscauda* sp. nov. clustered with *P. dyscrita*, *P. moskalevi*, and *P. raripes* (ML 92, BI 0.94), was a sister to *P. nigrimargaria* sp. nov. with high support (ML 99, BI 1), then followed by *P. pawsoni* with full support (ML

100, BI 1); and ~~clade~~ 3: *P. asperatus* sp. nov. clustered with *P. verrucicaudatus* (ML 97, BI 0.97) and was a sister to the only species of *Psycheotrephes*, *P. exigua* Théel, 1882 (ML 99, BI 1).

Discussion

Generic assignment, species delineation, and taxonomic characters

Both the morphology and molecular phylogenetic analyses supported the assignment of the three new species to the genus *Psychropotes*. The external morphological features (i.e., absence of ventral anus and circum-oral papillae) in *Psychropotes* species were most similar to species of *Psycheotrephes*. However, *Psychropotes* had unpaired dorsal appendages, which were absent in *Psycheotrephes*. The three new species in this study conformed to this unique feature, so they all belonged to *Psychropotes*. *P. asperatus* sp. nov., *P. diutiuscauda* sp. nov., and *P. nigrimargaria* sp. nov. were separated from other congeners by dorsal ossicle types, the length and position of unpaired dorsal appendages, and the number of ventrolateral tube feet.

The inter- and intraspecific genetic divergences of the COI were calculated to investigate the genetic distances in *Psychropotes*. For the COI alignment, the intraspecific distances ranged from 0.00 to 1.23%, and the interspecific distances were in the range of 1.38–13.24%. The minimum interspecific distance seemed low, but *Bribiesca-Contreras et al. (2022)* confirmed that the COI gene seemed to be more conserved in the genus *Psychropotes* (1.1–13.4%), and the interspecific divergence between some species pairs was < 2% (e.g., the genetic distances between *P. dyscrita* and *P. moskalevi* were 1.38–2.64% in this study, and the genetic distances were 1.1 ± 0.4% in *Bribiesca-Contreras et al. (2022)*. The genetic distances between *P. asperatus* sp. nov. and congeners were in the range of 3.14–13.05%, between the new species *P. diutiuscauda* sp. nov. and congeners in the range of 1.56–12.65%, and between *P. nigrimargaria* sp. nov. and congeners in the range of 2.84–12.38%. These divergences were higher than the known intraspecific variation in *Psychropotes* species (0.00–1.23%), which supported the distinction between the three new species and other congeners.

The discovery of two new species, *Psychropotes diutiuscauda* sp. nov., and *P.*

nigrimargaria sp. nov., increased the number of the psychropotid holothurians with long dorsal appendages placed close to or at a short distance from the posterior body end to 10 species: *P. diutiuscauda* sp. nov., *P. dubiosa*, *P. dyscrita*, *P. fuscopurpurea*, *P. longicauda*, *P. monstrosa*, *P. moskalevi*, *P. nigrimargaria* sp. nov., *P. pawsoni*, and *P. raripes*. In addition, *P. diutiuscauda* sp. nov. was the fourth reported yellowish-green psychropotid holothurian besides *P. dyscrita*, *P. moskalevi*, and *P. xenochromata*. *Psychropotes xenochromata* was discovered as the first yellow-green species, which was unusual for this genus. However, it was later found that the species in the genus *Psychropotes*, especially the long-tailed species, had diverse colors, and the colors of living specimens ranged from purple/violet to yellow/green/brown (*Gebruk, Kremenetskaia & Rouse, 2020*).

Thus, even in the living state, only preliminary identification can be made using body color, and body color cannot be used as the most effective morphological character for species identification. In addition, the length of the dorsal papillae, and the bifurcated or single-pointed dorsal appendages were not the most striking and recognizable characteristics of *Psychropotes* (*Hansen, 1975*; *Xiao, Li & Sha, 2018*). In this study, we made a taxonomic key by reviewing morphologically similar features of each species and different features that distinguished them from other congeners. In addition to the stable morphological features of ossicle types, external morphological features were used to identify species, which included the number of dorsal papillae, the presence or absence of free ventrolateral tube feet, the number of ventrolateral tube feet, and the length and position of the dorsal appendages.

Geographical distribution of psychropotid species

Based on the analysis of available data from OBIS and GBIF, the world distribution of psychropotid species is as follows. In total, there are three genera and 44 species in the family Psychropotidae, which include the three new species described here, 27 of which are distributed in the Pacific Ocean (i.e., 13 species in *Psychropotes*, 11 species in *Benthodytes*, three species in *Psycheotrephes*), 12 species in the Indian Ocean (i.e., nine species in *Psychropotes* and three species in *Benthodytes*), six species in the Atlantic Ocean (i.e., two species in *Psychropotes* and four species in *Benthodytes*), and only one species in the Antarctic (i.e., *Psycheotrephes recta*).

Twenty-two species, which include three new species, in the genus *Psychropotes* are distributed widely, with a depth range of 957–7250 m. *P. verrucosa* has the deepest record in the genus (depth 7250 m), and *P. depressa* has the shallowest record (depth 957 m). Thirteen species of *Psychropotes* were discovered in the deep water of the Pacific Ocean, and five of those species were recorded from the South Pacific Ocean: *P. asperatus* sp. nov., *P. depressa*, *P. longicauda*, *P. loveni*, and *P. verrucosa.* Seven species are only distributed in the Indian Ocean: *P. belyaevi*, *P. diutiuscauda* sp. nov., *P. fuscopurpurea*, *P. nigrimargaria* sp. nov., *P. minuta*, *P. mirabilis*, and *P. xenochromata*. Two other species, *P. scotiae* and *P. semperiana*, are distributed mainly in the Atlantic and Indian Ocean. Among the four valid species of the genus *Psycheotrephes*, three were recorded from the Pacific region (Fig. 16), and *Psycheotrephes recta* (*Vaney, 1908*) is the only species distributed in the Antarctic (specific data not available). The depth range of *Psycheotrephes* is 4182–5029 m. There are 18 species in the genus *Benthodytes*, four of which were found only in the Atlantic: *Benthodytes gosarsi* Gebruk, 2008, *B. lingua* Perrier R., 1896, *B. valdiviae* Hansen, 1975, and *B. violeta* Martinez, Solis-Marin & Penchaszadeh, 2014. Three species are distributed only in the Indian Ocean: *B. plana* Hansen, 1975, *B. superba* Koehler & Vaney, 1905, and *B. wolffi* Rogacheva & Cross in Rogacheva et al., 2009. The remaining species were found mainly in the Pacific Ocean. *Benthodytes sibogae* Sluiter, 1901 and *B. marianensis* Li, Xiao, Zhang & Zhang, 2018 were collected from the shallowest (694 m) and deepest (5567 m) depths recorded for this genus, respectively, with depth information based on specimens collected in the Mariana Trench and the South China Sea (*Li et al., 2018*; *Xiao, Xiao & Zeng, 2020*).

Overall, species in the family Psychropotidae span a wide range of depths (694–7250 m), which extend from bathyal depths ~~(300–2000 m)~~ to the hadal zone ~~(6000–11000 m).~~ Such high species richness and wide geographical distribution indicate that there are likely more species to be discovered in the Pacific Ocean. There is no doubt that it is necessary to conduct more investigations of deep-sea holothurians in different areas to unravel their taxonomy and phylogeny.

Conclusions

We described a new species (*Psychropotes asperatus* sp. nov.) and one new record (*Psychropotes depressa*) from the Kermadec Trench region in the South Pacific Ocean, and two new species (*Psychropotes diutiuscauda* sp. nov. and *Psychropotes nigrimargaria* sp. nov.) from the WZFZ in the East Indian Ocean. We developed an dichotomous key for *Psychropotes.* The yellow-green body color, the size of the dorsal papillae, and unpaired dorsal appendages that were single-pointed or divided in varying degrees at the tip could not be used as unique identification features to distinguish the species. The key morphological features were the number of dorsal papillae, the number of free ventrolateral tube feet, the length and position of the unpaired dorsal appendages, and the ossicle types. Phylogenetic analyses showed that the family Laetmogonidae is polyphyletic, and the genus *Benthodytes* in the family Psychropotidae is paraphyletic. The family Psychropotidae exhibits a broad geographical range, with the Pacific Ocean displaying the greatest variety of species, hosting 27 out of the 44 recognized species.

Acknowledgements

We thank the crew of the vessel ‘Tansuo 2’ and the HOV team ‘Fendouzhe’ for their assistance in the collection of the specimens. We appreciate the scientists from IDSSE and NIWA for their help in taking photographs of fresh specimens before fixation. Many thanks to Prof. Xiaotong Peng group for providing the gold spraying service and Prof. Shenghua Mei group for electron microscope support. We are grateful to Dr. Ashley Rowden, Dr. Daniel Leduc, and Ms. Caroline Chin from NIWA for their constructive comments on the manuscript.

References

Alfaro ME, Zoller S, Lutzoni F. 2003. Bayes or Bootstrap? A simulation study comparing the performance of Bayesian Markov chain Monte Carlo sampling and bootstrapping in assessing phylogenetic confidence. *Molecular Biology & Evolution* **20(2)**: 255–226 DOI 10.1093/molbev/msg028.

~~**Benham WB. 1912.** Report on sundry invertebrates from the Kermadec Islands. *Transactions & Proceedings of the New Zealand Institute (for 1911)* **44(12)**: 135–138.~~

~~**Bond T, Niyazi Y, Kolbusz JL, Jamieson AJ. 2023.** Habitat and benthic fauna of the Wallaby-Cuvier escarpment, SE indian ocean. *Deep-sea research, Part II. Topical studies in oceanography* **210(Aug.)**: 105299 DOI https://doi.org/10.1016/j.dsr2.2023.105299.~~

Bribiesca-Contreras G, Dahlgren TG, Amon DJ, Cairns S, Drennan R, Durden JM, Eléaume MP, Hosie AM, Kremenetskaia A, McQuaid K, O'hara TD, Rabone M, Simon-Lledó E, Smith CR, Watling L, Wiklund H, Glover AG. 2022. Benthic megafauna of the western Clarion-Clipperton Zone, Pacific Ocean. *ZooKeys* **1113:** 1–110 DOI 10.3897/zookeys.1113.82172.

Clark AH. 1920. Echinoderms. Report of the Canadian Arctic Expedition 1913–1918. Vol. VIII. *Mollusks, Echinoderms, Coelenterates, etc. Part C: Echinoderms*: 1–13 DOI 10.5962/bhl.title.64183.

Deichmann E. 1930. The holothurians of the western part of the Atlantic Ocean. *Memoirs of the Museum of Comparative Zoology (Harvard)* **71:** 41–226.

Deichmann E. 1940. Report on the holothurians, collected by the Harvard-Havana expeditions 1938 and 1939, with a revision of the Molpadonia of the Atlantic Ocean. *Memorias de la Sociedad Cubana de Historia Natural* **14:** 183–240.

Deichmann E. 1954. The holothurians of the Gulf of Mexico. *Fishery Bulletin of the Fish and Wildlife Service* **55(89):** 381–410.

Ekman S. 1926. Systematisch-phylogenetische Studien uber Elasipoden und Aspidochiroten. *Zoologische Jahrbücher, Abteilung Algemeine Zoologie Physiologie Tiere* **47:** 429–540.

Eakins BW, Sharman GF. 2010. Volumes of the World's Oceans from ETOPO1. Boulder, CO: NOAA National Geophysical Data Center. *Available at: http://www.ngdc.noaa.gov/mgg/global/etopo1_ocean_volumes.html.*

Gascuel O. 2010. New Algorithms and Methods to Estimate Maximum-Likelihood Phylogenies: Assessing the Performance of PhyML 3.0. *Systematic Biology* **59:** 307–321 DOI 10.1093/sysbio/syq010.

Gebruk AV. 2008. Holothurians (Holothuroidea, Echinodermata) of the northern Mid-Atlantic Ridge collected by the G.O. Sars MAR-ECO expedition with descriptions of four new species. *Marine Biology Research* **4(1-2):** 48–60 DOI 10.1080/17451000701842898.

Gebruk AV, Kremenetskaia A, Rouse GW. 2020. A group of species "*Psychropotes longicauda*" (Psychropotidae, Elasipodida, Holothuroidea) from the Kuril-Kamchatka Trench area (North-West Pacific). *Progress in Oceanography* **180:** 102222 DOI 10.1016/j.pocean.2019.102222.

Grieg JA. 1921. Echinodermata. *Report on the Scientific Results of the Michael Sars North Atlantic Deep-Sea Expedition* **3:** 1–47 DOI: 10.5962/bhl.title.79346.

Hansen B. 1975. Scientific results of the Danish Deep-Sea Expedition Round the World 1950–52. Systematics and biology of the deep-sea holothurians. Part 1: Elasipoda. *Galathea Report* **13:** 1–262.

Hérouard E. 1902. Holothuries provenant des campagnes de la Princesse Alice (1892–1897). *Résultats des Campagnes Scientifiques Accomplies sur son yacht par Albert Ier Prince Souverain de Monaco* **21:** 1–61.

Heding SG. 1940. Die Holothurien der deutschen Tiefsee-Expedition. II Aspidochirote und Elasipode Formen. Wissenschaftliche Ergebnisse der Deutschen. *Tiefsee-Expedition auf dem Dampfer Valdivia 1898–1899* **24:** 317–375.

Heding SG. 1942. Holothurioidea. II. *Danish Ingolf-Expedition* **4(13):** 1–39.

Hillis DM, Bull JJ. 1993. A Empirical Test of Bootstrapping as a Method to Assess Confidence in Phylogenetic Analysis. *Systematic Biology* **42:** 182–192 DOI 10.1093/sysbio/42.2.182

Janßen F, Treude T, Witte U. 2000. Scavenger assemblages under differing trophic conditions: A case study in the deep Arabian Sea. *Deep-Sea Research Part II: Topical Studies in Oceanography* **47:** 2999–3026 DOI 10.1016/S0967-0645(00)00056-4.

Jamieson AJ, Gebruk A, Fujii T, Solan M. 2011. Functional effects of the hadal sea cucumber Elpidia atakama (Echinodermata: Holothuroidea, Elasipodida) reflect small-scale patterns of resource availability. *Marine Biology* **158:** 2695–2703 DOI 10.1007/s00227-011-1767-7

Jamieson AJ, Stewart HA, Rowden AA, Clark MR. 2020. Geomorphology and benthic habitats of the Kermadec Trench, Southwest Pacific Ocean. In Peter T. Harris, Elaine Baker, eds. *Seafloor Geomorphology as Benthic Habitat*. Amsterdam: Elsevier, 949–966 DOI 10.1016/B978-0-12-814960-7.00059-2.

Jamieson AJ, Stewart HA, Weston JNJ, Lahey P, Vescovo VL. 2022. Hadal Biodiversity, Habitats and Potential Chemosynthesis in the Java Trench, Eastern Indian Ocean. *Frontiers in Marine Science* **9:** 1–15 DOI 10.3389/fmars.2022.856992.

Jamieson AJ, Giles GT, Stewart HA. 2024. Hadal zones of the Southwest Pacific and east Indian oceans. *Marine Geophysical Research* **45(3):** 17 DOI: 10.1007/s11001-024-09550-7.

Katoh K, Standley D. 2013. MAFFT Multiple Sequence Alignment Software Version 7: Improvements in performance and usability. *Molecular Biology and Evolution* **30(4):** 772–780 DOI 10.1093/molbev/mst010.

Keable SJ, Reid AL. 2015. Marine Invertebrates Collected during the Kermadec Biodiscovery Expedition 2011. *Bulletin of the Auckland Museum* **20:** 115–137.

Koehler R, Vaney C. 1905. An Account of the Deep-Sea Holothuroidea Collected by the Royal Indian Marine Survey Ship Investigator. The Indian Museum, Calcutta, 170 pp DOI 10.5962/bhl.title.1730.

Kremenetskaia A, Gebruk A, Alt CHS, Budaeva N. 2021. New and poorly known species of *Peniagone* (Holothuroidea, elpidiidae) from the Northwest Pacific Ocean with Discussion on Phylogeny of the genus. *Diversity* **13(11):** 541 DOI 10.3390/d13110541.

Kumar S, Stecher G, Li M, Knyaz C, Tamura K. 2018. MEGA X: Molecular Evolutionary

Genetics Analysis across Computing Platforms. *Molecular Biology and Evolution* **35(6)**: 1547–1549 DOI 10.1093/molbev/msy096.

Lam-Tung N, Schmidt HA, Arndt VH, Quang MB. 2015. IQ-TREE: A Fast and Effective Stochastic Algorithm for Estimating Maximum-Likelihood Phylogenies. *Molecular Biology & Evolution* **32(1)**: 268–274 DOI 10.1093/molbev/msu300.

Lanfear R, Frandsen PB, Wright AM, Senfeld T, Calcott B. 2017. PartitionFinder 2: New Methods for Selecting Partitioned Models of Evolution for Molecular and Morphological Phylogenetic Analyses. *Molecular Biology & Evolution* **34(3):** 772–773 DOI 10.1093/molbev/msw260.

Lee S, Ferse S, Ford A, Wild C, Mangubhai S. 2017. Effect of sea cucumber density on the health of reef-flat sediments. In: Mangubhai S, Lalavanua W, and Purcell SW. *Fiji's Sea Cucumber Fishery: Advances in Science for Improved Management*. Suva: Wildlife Conservation Society, 54–61.

Li YN, Xiao N, Zhang LP, Zhang H. 2018. *Benthodytes marianensis*, a new species of abyssal elasipodid sea cucumbers (Elasipodida: Psychropotidae) from the Mariana Trench area. *Zootaxa* **4462(3):** 443–450 DOI 10.11646/zootaxa.4462.3.10.

Ludwig H. 1893. Vorläufiger bericht über die erbeuteten holothurien. Reports on the Dredging Operations off the West Coast of Central America to the Galapagos, etc., by the U.S. Fish Commission Steamer "*Albatross*". IV. *Bulletin of the Museum of Comparative Zoöology at Harvard College* **24(4):** 105–114.

Ludwig H. 1894. The Holothurioidea. Reports on an exploration off the west Coast of Mexico, Central and South America, and off Galapagos Islands, in Charge of Alexander Agassiz. by the U.S. Fish Commission Steamer "*Albatross* " during 1891. *Memoirs of the Museum of Comparative Zoology at Harvard College* **17:** 1–183.

Madsen FJ. 1947. The echinoderms collected by the Skagerak expedition in the Eastern Atlantic 1946. 1. Asteroidea: Ophiuroidea: Echinoidea: Holothuroidea. *Göteborgs Kungliga Vetenskaps-och Vitterhets Samhälles Handlingar Serie B* **5(7):** 1–16.

Martinez MI, Solís-Marín FA, Penchaszadeh PE. 2014. *Benthodytes violeta*, a new species of a deep-sea holothuroid (Elasipodida: Psychropotidae) from Mar del Plata Canyon (south-western Atlantic Ocean). *Zootaxa* **3760(1):** 89 DOI 10.11646/zootaxa.3760.1.6.

Miller AK, Kerr AM, Paulay G, Reich M, Wilson NG, Carvajal JI, Rouse GW. 2017. Molecular phylogeny of extant Holothuroidea (Echinodermata). *Molecular Phylogenetics and Evolution* **111:** 110–131 DOI 10.1016/j.ympev.2017.02.014.

Minh BQ, Nguyen MAT, Haeseler A Von. 2013. Ultrafast Approximation for Phylogenetic Bootstrap. *Molecular Biology and Evolution* **30:** 1188–1195 DOI 10.1093/molbev/mst024.

Ogawa A, Kobayashi I, Kohtsuka H, Fujita T. 2023. Two new species of the bathyal holothurian genus *Pannychia* (Elasipodida, Laetmogonidae) from Japanese waters. *Zootaxa* **5323:** 105–125 DOI 10.11646/zootaxa.5323.1.6.

Ogawa A, Kremenetskaia A, Hiruta SF, Shibata Y, Narimatsu Y, Miki S, Morita T, Tsuchida S, Fujiwara Y, Fujita T. 2022. Rehabilitation of two deep-sea holothurian species in genus *Pannychia* from the northwest Pacific Ocean. *Deep-Sea Research Part II: Topical Studies in Oceanography* **202:** 105099 DOI 10.1016/j.dsr2.2022.105099.

Ohshima H. 1915. Report on the holothurians collected by the United States fisheries steamer Albatross in the Northwestern Pacific during the summer of 1906. *Proceedings of the United States National Museum*. **48:** 213–291 DOI 10.5479/si.00963801.48-2073.213.

O'Loughlin PM, Paulay G, Davey N, Michonneau F. 2011. The Antarctic region as a marine biodiversity hotspot for echinoderms: Diversity and diversification of sea cucumbers. *Deep-Sea Research Part II: Topical Studies in Oceanography* **58:** 264–275 DOI 10.1016/j.dsr2.2010.10.011.

O'Loughlin PM, Vandenspiegel D. 2012. Sea cucumbers collected by the Kermadec Biodiscovery Expedition 2011 (Echinodermata: Holothuroidea: Apodida and Dendrochirotida). *Zootaxa* **3515:** 60–66 DOI 10.11646/zootaxa.3515.1.4.

Parulekar AH, Harkantra SN, Ansari ZA, Matondkar SGP. 1982. Abyssal benthos of the central Indian Ocean. *Deep Sea Research Part A, Oceanographic Research* **29:** 1531–1537

DOI 10.1016/0198-0149(82)90041-3.

Pawson DL. 1985. *Psychropotes hyalinus*, new species, a swimming elasipod sea cucumber (Echinodermata: Holothuroidea) from the north central Pacific Ocean. *Proceedings of the Biological Society of Washington* **98(2):** 523-525.

Pavithran S, Ingole BS, Nanajkar M, Raghukumar C, Nath BN, Valsangkar AB. 2009. Composition of macrobenthos from the Central Indian Ocean Basin. *Journal of Earth System Science* **118:** 689–700 DOI 10.1007/s12040-009-0051-4.

Perrier R. 1896. Sur les Élasipodes recueillis par le Travailleur et le Talisman. *Comptes rendus hebdomadaires des séances de l'Académie des sciences* **123(21):** 900–903.

Perrier R. 1902. Holothuries. *Expéditions scientifiques du Travailleur et du Talisman pendant les années 1880, 1881, 1882, 1883*, Paris, 273–554.

Peng X, Zhang W, Schnabel K, Leduc D, Xu H, Zhang H, Zhang H, Rowden A. 2023. Unveiling the mysteries of the Kermadec Trench. *The Innovation* **4:**100367. DOI 10.1016/j.xinn.2022.100367.

Rogacheva A, Cross IA, Billett DSM, Shirshov PP. 2009. Psychropotid holothurians (Echinodermata: Holothuroidea: Elasipodida) collected at abyssal depths from around the Crozet Plateau in the Southern Indian Ocean. *Zootaxa* **2096(2096):** 460–478 DOI 10.11646/zootaxa.2096.1.28.

Post A, Przeslawski R, Huang Z, Smith D, Kirkendale L. 2021. An eco-narrative of Gascoyne Marine Park, North-west marine region. Report to the National Environmental Science Program, Marine Biodiversity Hub. Geoscience Australia, Canberra. Pushcharovsky, Y.M., 2007. Tectonic types of deepwater basins in the Indian Ocean. *Geotectonics* **41:** 355–367 DOI 10.1134/S0016852107050020.

Rambaut A. 2018. FigTree v1.4.4, a graphical viewer of phylogenetic trees. University of Edinburgh: Institute of Evolutionary Biology.

Rogacheva A, Gebruk A, Alt CHS. 2013. Holothuroidea of the Charlie Gibbs Fracture Zone area, northern Mid-Atlantic Ridge. *Marine Biology Research* **9:** 587–623 DOI

10.1080/17451000.2012.750428.

Ronquist F, Teslenko M, van der Mark P, Ayres DL, Darling A, Höhna S, Larget B, Liu L, Suchard MA HJ. 2012. MrBayes 3.2: Efficient Bayesian Phylogenetic Inference and Model Choice Across a Large Model Space. *Systematic Biology* **61:** 539–542 DOI 10.1093/sysbio/sys029.

Sluiter CP. 1901a. Neue holothurien aus der Tiefsee des Indischen Archipels Gesammelt durch die Siboga-Expedition. *Tijdschrift der Nederlandsche Dierkundige Vereeniging* **7(1):** 1–28.

Sluiter CP. 1901b. Die Holothurien der Siboga-Expedition. *Biodiversity Heritage Library OAI Repository* **44:** 1–142 DOI 10.5962/bhl.title.85348.

Théel H. 1882. Report on the Holothuroidea. Part I. *Report of the scientific results of the voyage of H.M.S. Challenger, Zoology: Analysis of Complex Systems*, ZACS **4(13):** 1–176.

Théel H. 1886. Report on the Holothurioidea. Reports on the results of dredging, "Blake", 30. *Bulletin of the Museum of Comparative Zoölogy at Harvard College* **13(1):** 1–21.

Vaney MC. 1908. Les Holothuries recueillies par l'Expédition antarctique écossaise. *Zoologischer Anzeiger* **33:** 290–299.

Verrill AE. 1884. Notice of the Remarkable Marine Fauna occupying the Outer Banks off the Southern Coast of New England, No. 9. *American Journal of Science* **3(28):** 213–220 DOI 10.2475/ajs.s3-28.165.213.

Verrill AE. 1885. Results of the explorations made by the Steamer Albatross off the North-Eastern coast of the United States in 1883. A*nnual Report of the United States Commission of Fish and Fisheries, Washington* **11:** 503–699 DOI 10.5962/bhl.title.12059.

Wessel P, Smith W. 1995. The generic mapping tools (GMT) version 3.0. Technical Reference and Cookbook.

Weston JNJ, Peart RA, Jamieson AJ. 2020. Amphipods from the Wallaby-Zenith Fracture Zone, Indian Ocean: new genus and two new species identified by integrative taxonomy. *Systematics and Biodiversity* **18:** 57–78. DOI 10.1080/14772000.2020.1729891.

Weston JNJ, Peart RA, Stewart HA, Ritchie H, Piertney SB, Linley TD, Jamieson AJ.

2021. Scavenging amphipods from the Wallaby-Zenith Fracture Zone: Extending the hadal paradigm beyond subduction trenches. *Marine Biology* **168:** 1–14 DOI 10.1007/s00227-020-03798-4.

WoRMS. 2024. *Psychropotes* Théel, 1882. *Available at https://www.marinespecies.org/aphia.php?p=taxdetails&id=123532* (accessed 12 June 2024).

Xiao N, Li X, Sha Z. 2018. Psychropotid holothurians (Echinodermata: Holothuroidea: Elasipodida) of the tropical Western Pacific collected by the KEXUE expedition with description of one new species. *Marine Biology Research* **14(8):** 816–826 DOI 10.1080/17451000.2018.1546012.

Xiao N, Gong L, Kou Q, Li X. 2019. *Psychropotes verrucicaudatus*, a new species of deep-sea holothurian (Echinodermata: Holothuroidea: Elasipodida: Psychropotidae) from a seamount in the South China Sea. *Bulletin of Marine Science* **95:** 421–430 DOI 10.5343/bms.2018.0041.

Xiao Y, Xiao N, Zeng X. 2020. New records of a genus and a species of Psychropotidae (Echinodermata: Holothuroidea: Elasipodida) from the South China Sea. *Oceanologia et Limnologia Sinica* **51(03):** 644-648.

Xiao Y, Xiao N, Zeng X. 2023. *Benthodytes tetrapapillata* sp. nov., a new elasipodid sea cucumber (Elasipodida: Psychropotidae) from a seamount in the Western Pacific Ocean. *Journal of Oceanology and Limnology* **41(5):** 1978–1987 DOI 10.1007/s00343-022-2220-0.

Xiao Y, Xiao N, Zeng X. 2023. *Benthodytes tetrapapillata* sp. nov., a new elasipodid sea cucumber (Elasipodida: Psychropotidae) from a seamount in the Western Pacific Ocean. *Journal of Oceanology and Limnology* **41:** 1978–1987 DOI 0.1007/s00343-022-2220-0

Xiao Y, Zhang H. 2024. Integrative taxonomy reveals three new species and one new record of the genus *Psychropotes* (Echinodermata, Holothuroidea, Elasipodida) from the Kermadec Trench region and the Wallaby-Zenith Fracture Zone DOI 10.57760/sciencedb.10389

Yu C, Wang C, Zhang D, Zhang R. 2021. *Benthodytes palauta*, a new species of deep-sea holothuroid (Elasipodida: Psychropotidae) from the western Pacific Ocean. *Acta Oceanologica Sinica* **40:** 50–54 DOI 10.1007/s13131-021-1937-5.

Yu C, Zhang D, Zhang R, Wang C. 2022. New psychropotid species (Echinodermata, Holothuroidea, Elasipodida) of the Western Pacific with phylogenetic analyses. *ZooKeys* **2022:** 99–114 DOI 10.3897/zookeys.1088.69141.

Yuan C, Wang C, Zhang D. 2024. *Benthodytes occidentpalauta* sp. nov., a new species of deep-sea holothuroid (Elasipodida: Psychropotidae) from the west of Kyushu-Palau Ridge in the Western Pacific Ocean. *Journal of Oceanology and Limnology* **42:** 252–262 DOI 10.1007/s00343-023-2344-x.

Figure 1

Sampling locations of the studied *Psychropotes* species in the Kermadec Trench region and the Wallaby-Zenith Fracture Zone.

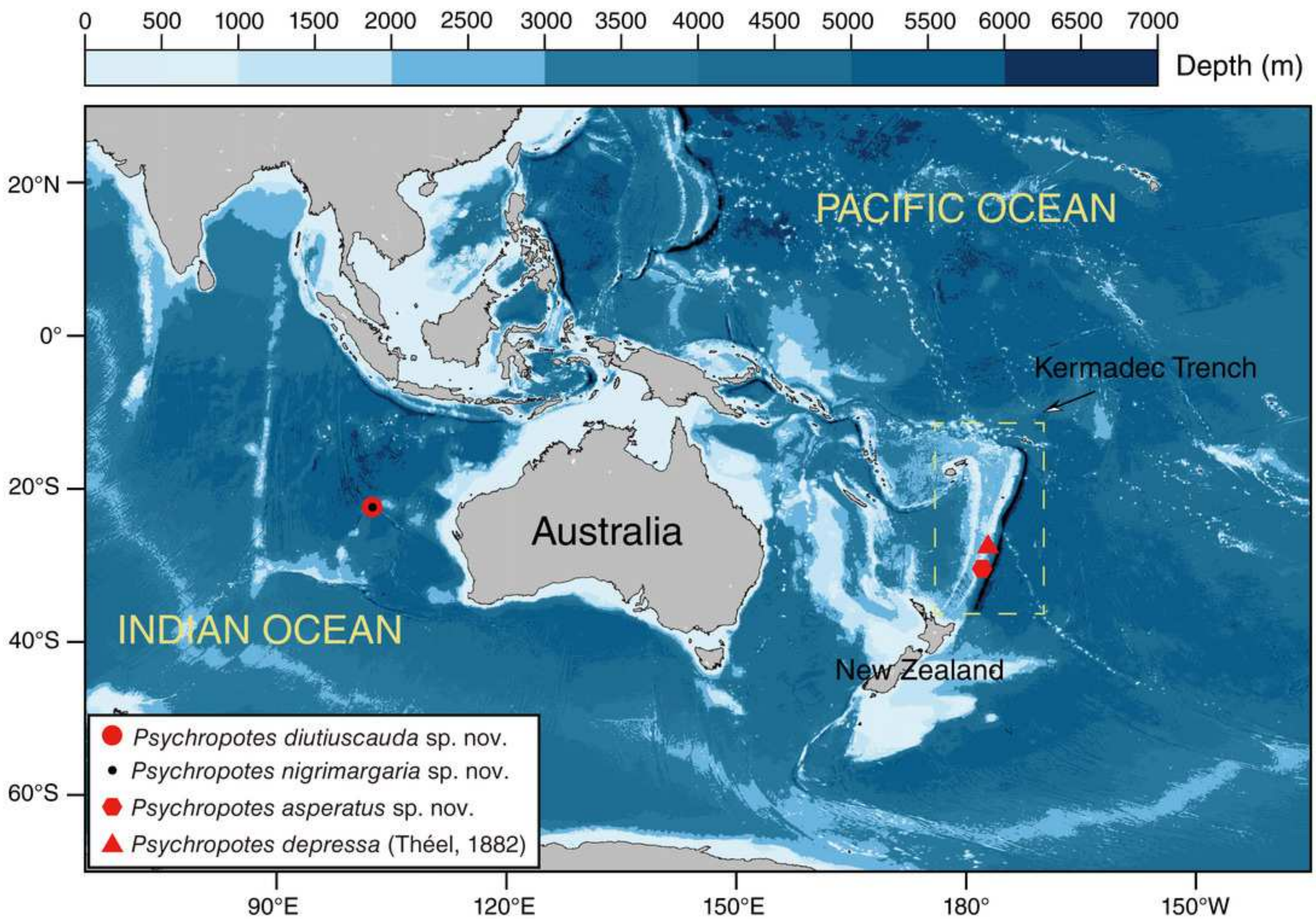

Figure 2

Psychropotes asperatus sp. nov., holotype (NIWA164003).

(A, B) The holotype specimen *in situ*. (C, D) The holotype in preserved state. (E) Dorsal warts. (F) Closeup shooting of warts on dorsum. Scale bars: 2 cm (C, D), 500 µm (E, F).

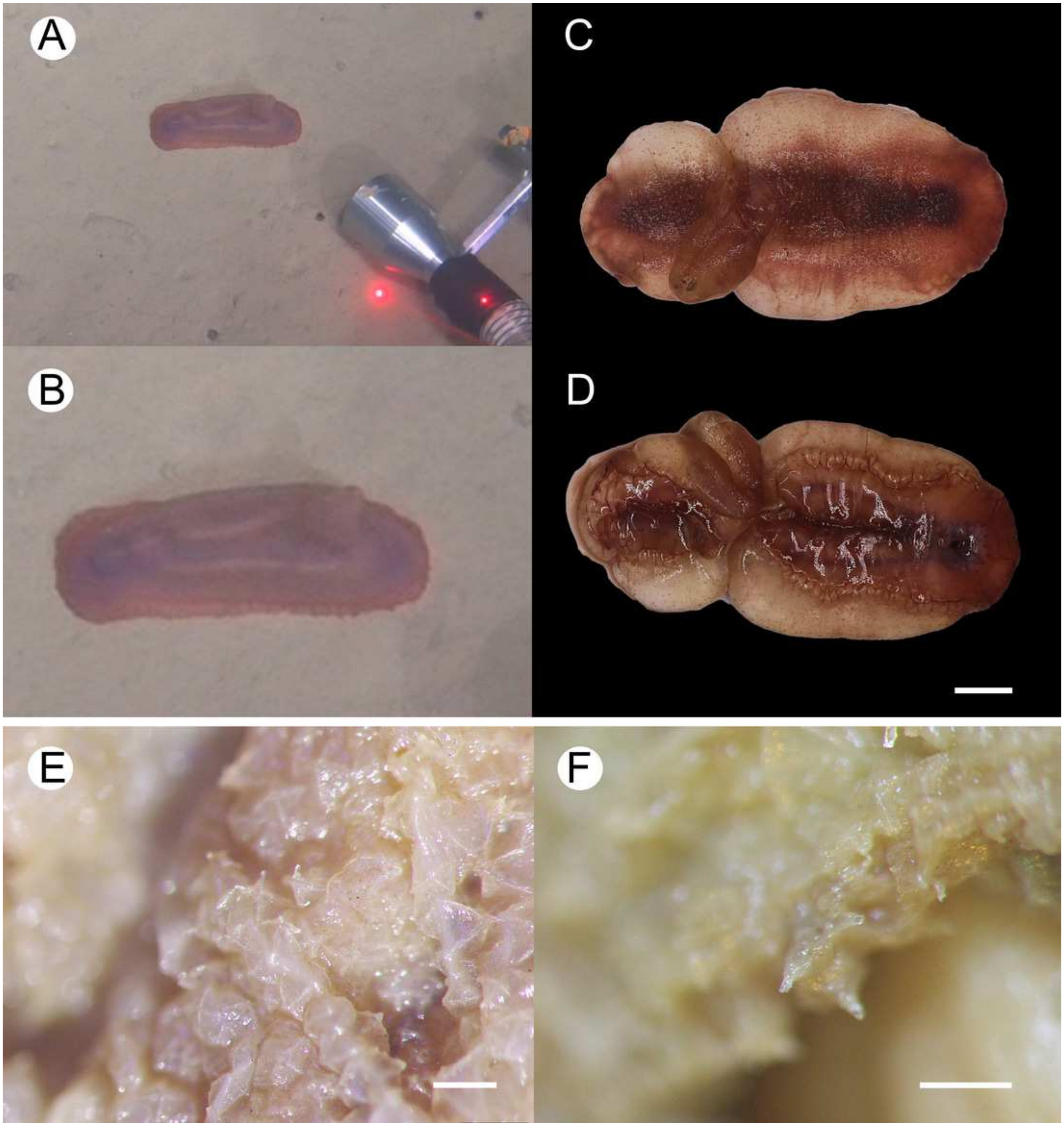
A
B
C
D
E
F

Figure 3

Psychropotes asperatus sp. nov., SEM, holotype (NIWA164003).

(A–F) Ossicles from dorsal body wall; (G–L) unpaired dorsal appendage. Scale bar: 300 µm.

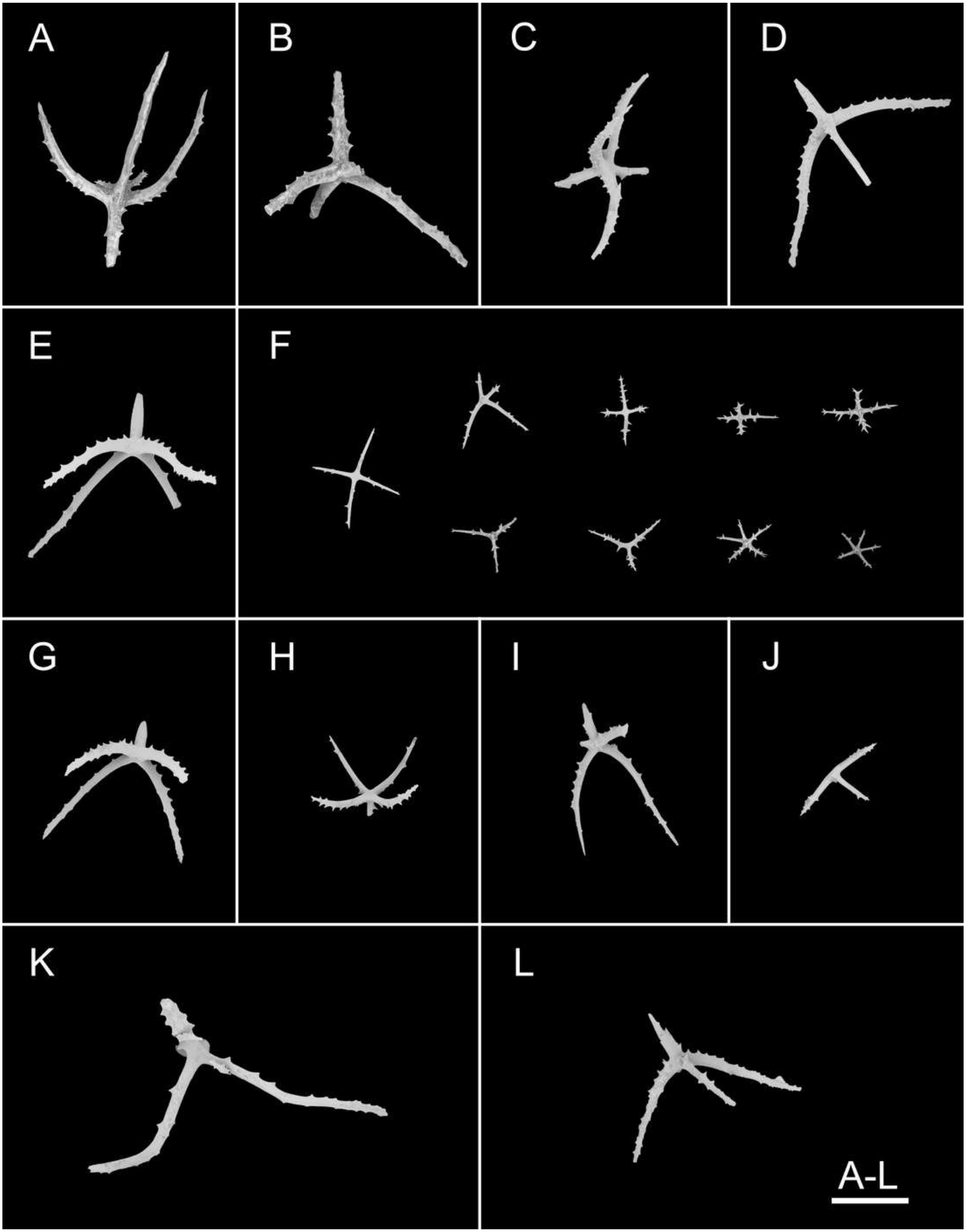
A
B
C
D
E
F
G
H
I
J
K
L
A-L

Figure 4

Psychropotes asperatus sp. nov., SEM, holotype (NIWA164003).

(A–D) Ossicles from tentacles; (E, F) tube feet; (G–J) ventral body wall. Scale bar: 300 µm.

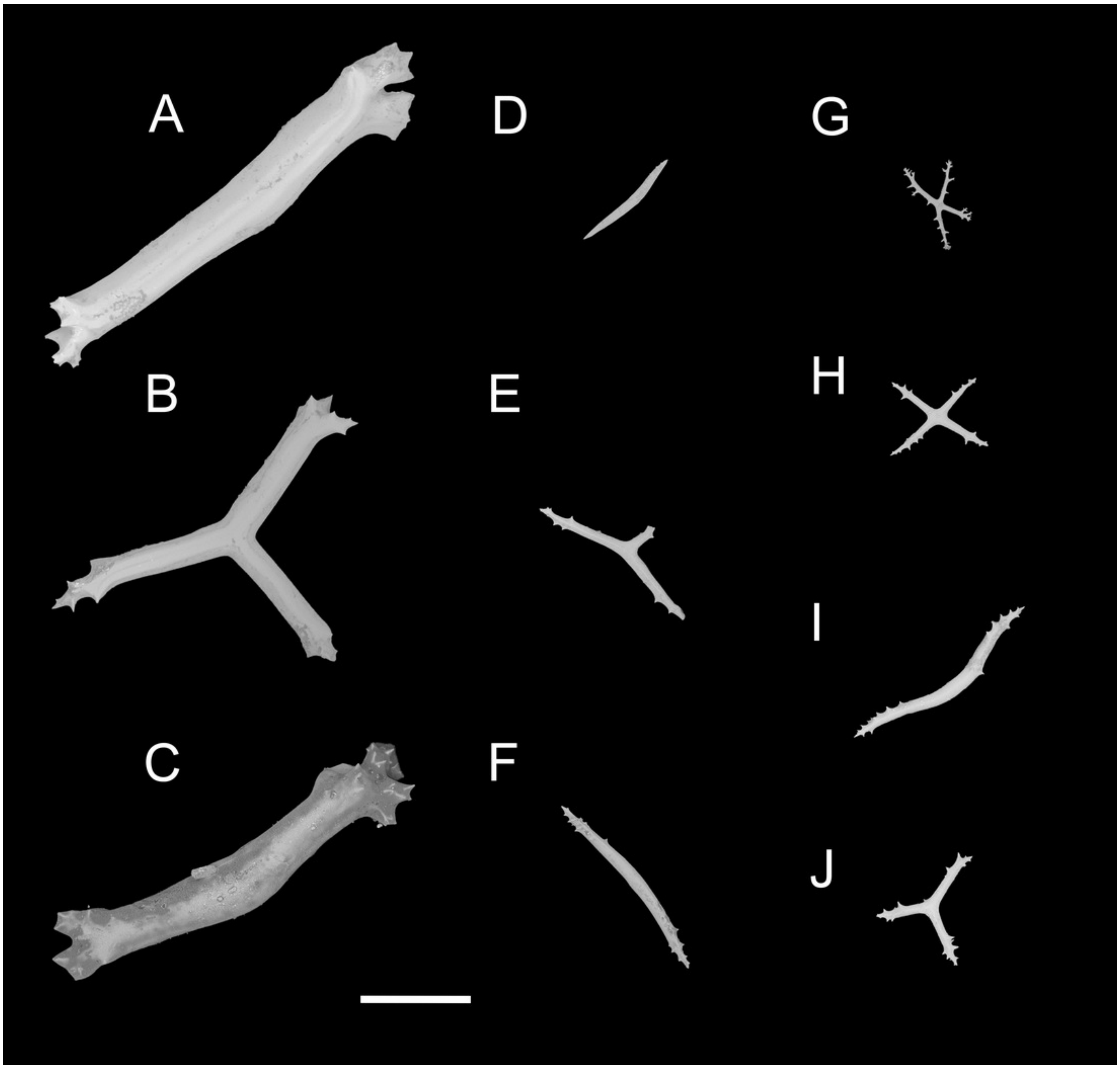

Figure 5

Psychropotes diutiuscauda sp. nov., holotype (FDZ188-F01).

(A, B) *In situ* images. (C) Specimen before fixation in absolute ethanol. (D, E) Preserved in absolute ethyl alcohol after a few days. Scale bars: the distance between the two laser points is 10 cm (A, B); 3 cm (C–E).

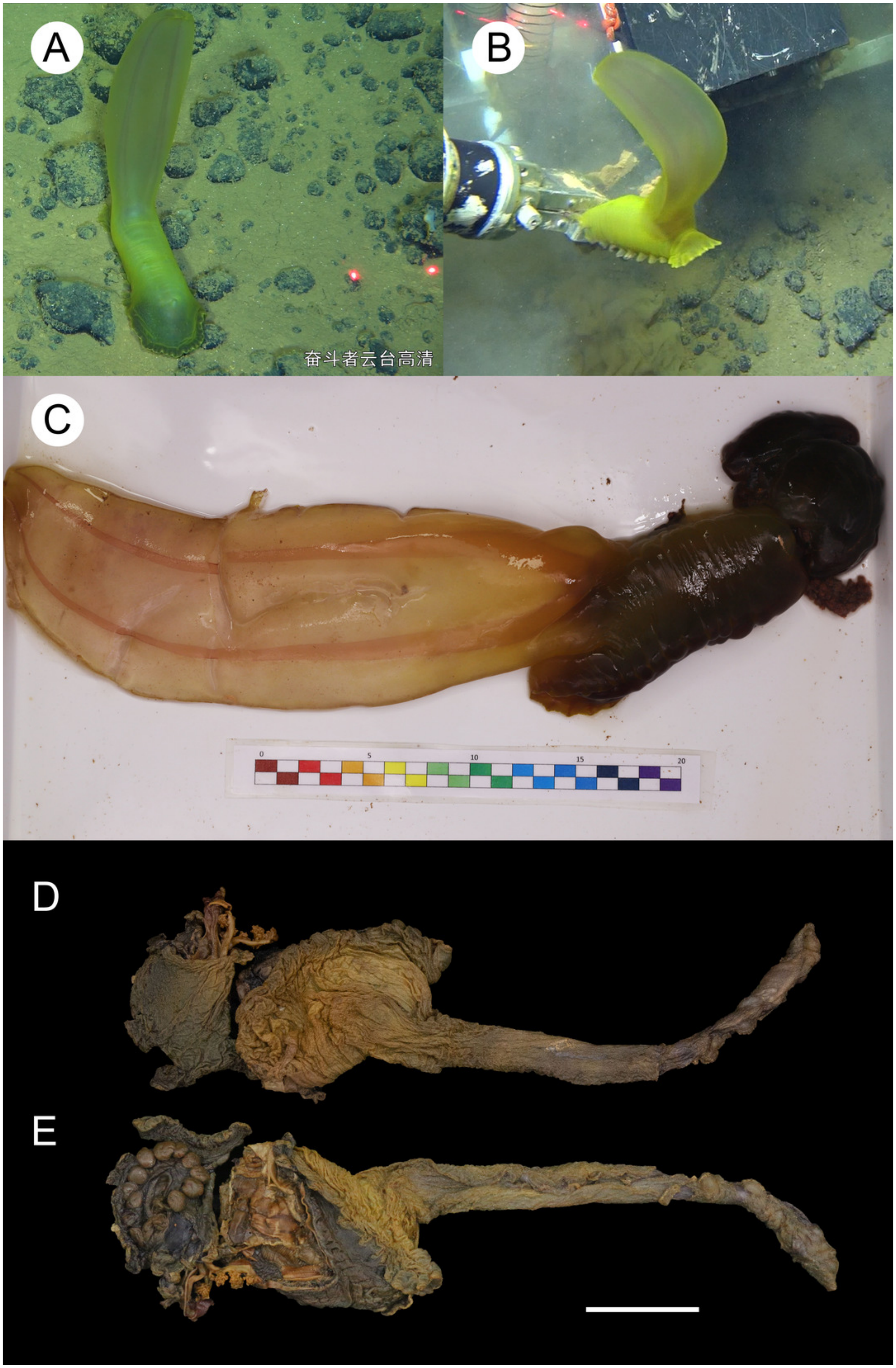
A
B
奋斗者云台高清
C
0
5
10
15
20
D
E

Figure 6

Psychropotes diutiuscauda sp. nov., SEM, holotype (FDZ188-F01).

(A–I) Ossicles from dorsal body wall. Scale bar: 100 µm.

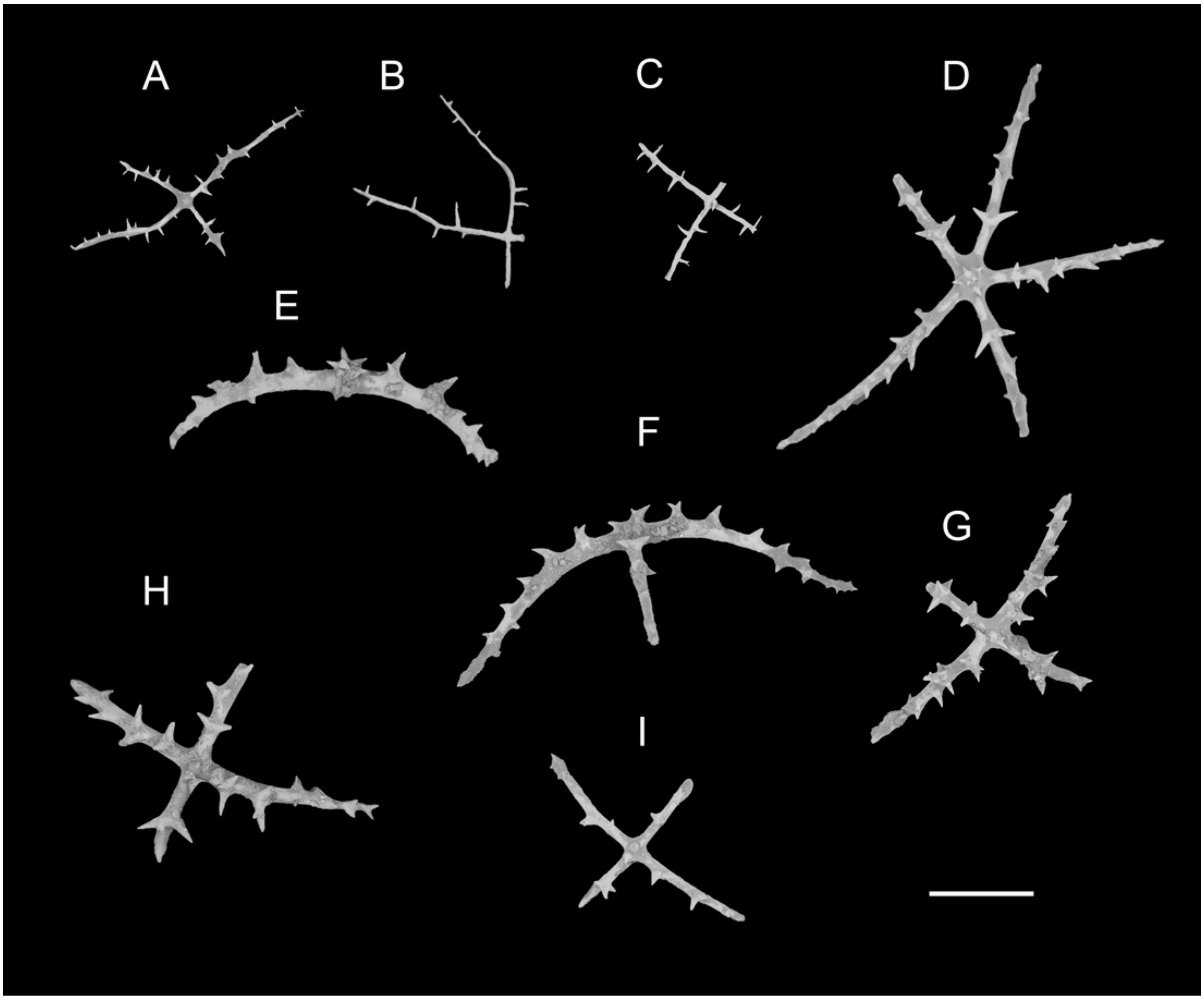

Figure 7

Psychropotes diutiuscauda sp. nov., SEM, holotype (FDZ188-F01).

(A–P) Ossicles from ventral body wall. Scale bar: 50 µm.

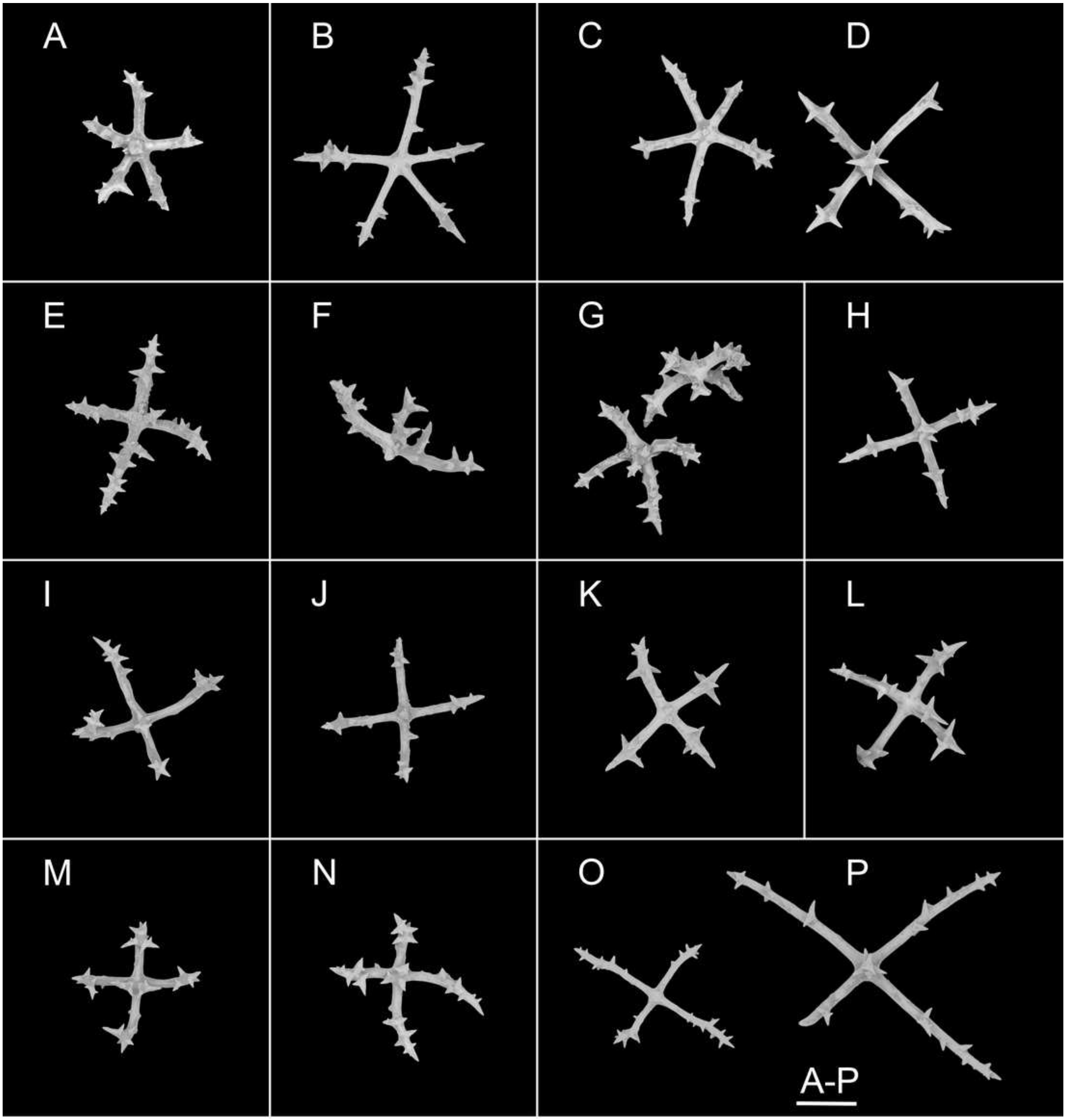
A
B
C
D
E
F
G
H
I
J
K
L
M
N
O
P
A-P

Figure 8

Psychropotes diutiuscauda sp. nov., SEM, holotype (FDZ188-F01).

(A–Q) Ossicles from tube feet; (R–V) tentacles. Scale bars: 100 µm.

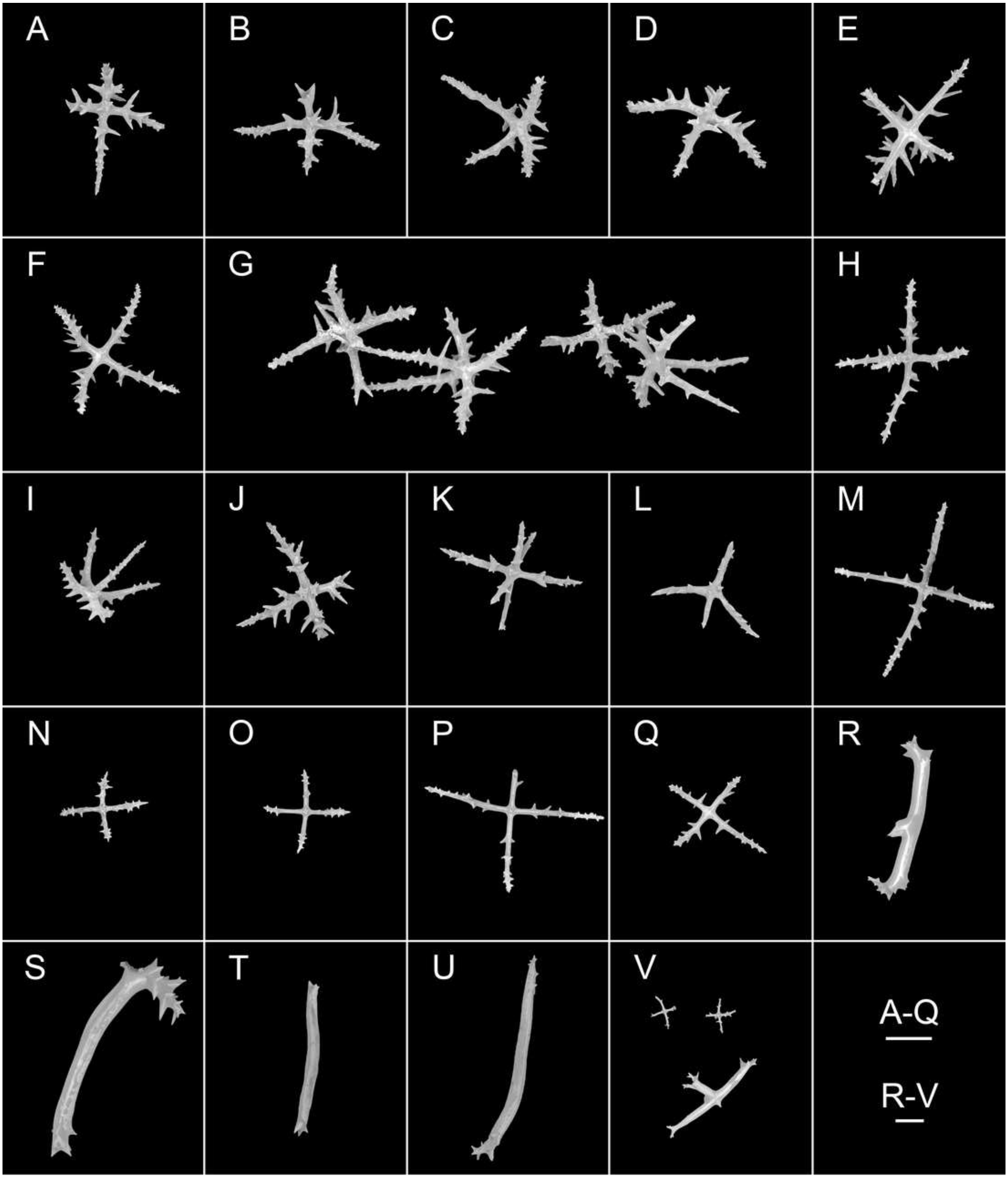
A
B
C
D
E
F
G
H
I
J
K
L
M
N
O
P
Q
R
S
T
U
V
A-Q
R-V

Figure 9

Psychropotes nigrimargaria sp. nov., holotype (FDZ188-F02).

(A, B) *In situ* images. (C) Specimen before fixation. (D, E) Specimen after preservation. Scale bars: 10 cm (A, B), 3 cm (C–E).

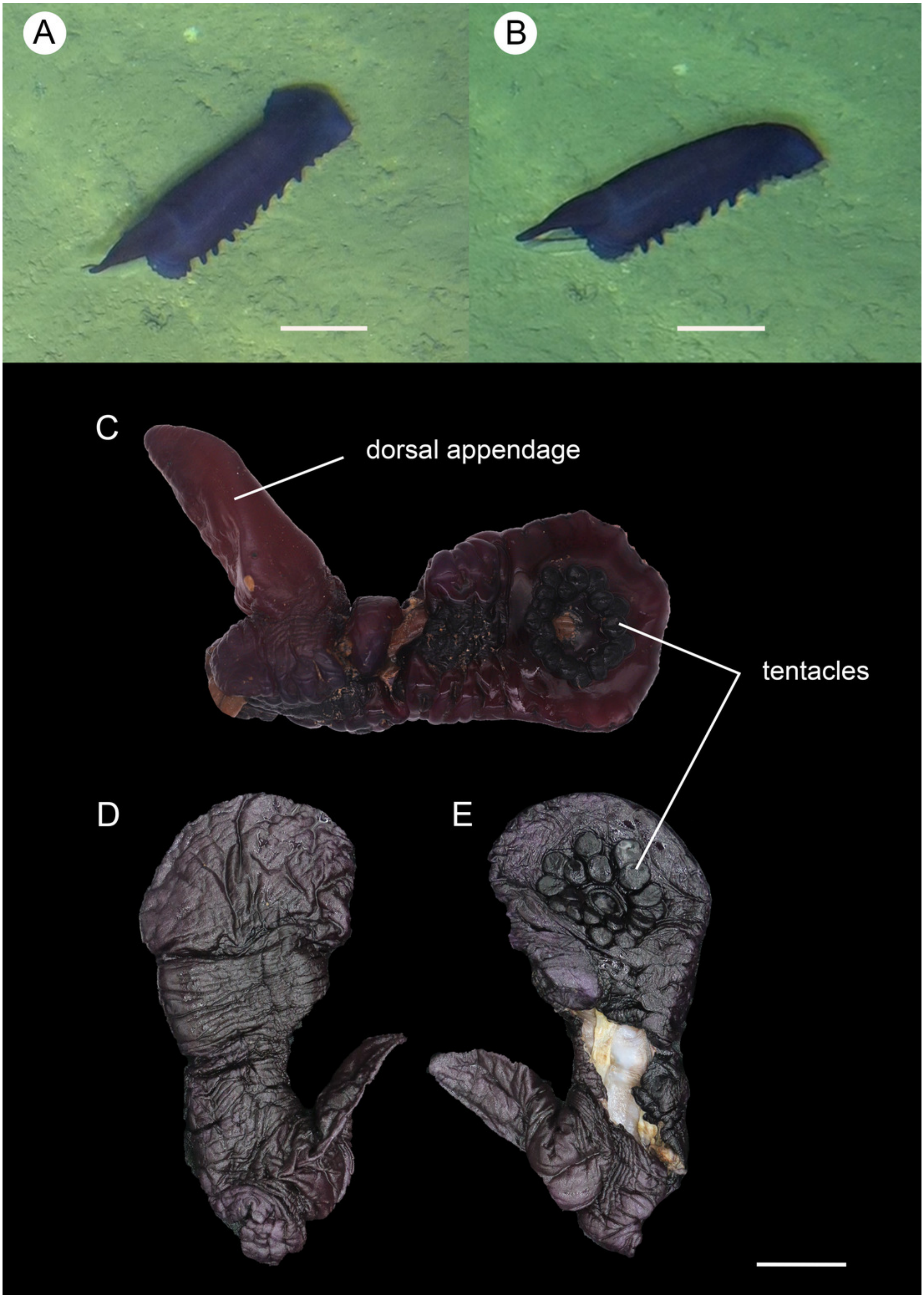
A
B
C
dorsal appendage
tentacles
D
E

Figure 10

Psychropotes nigrimargaria sp. nov., SEM, holotype (FDZ188-F02).

(A–G) Ossicles from dorsal body wall; (H–J) ventral body wall. Scale bars: 100 µm.

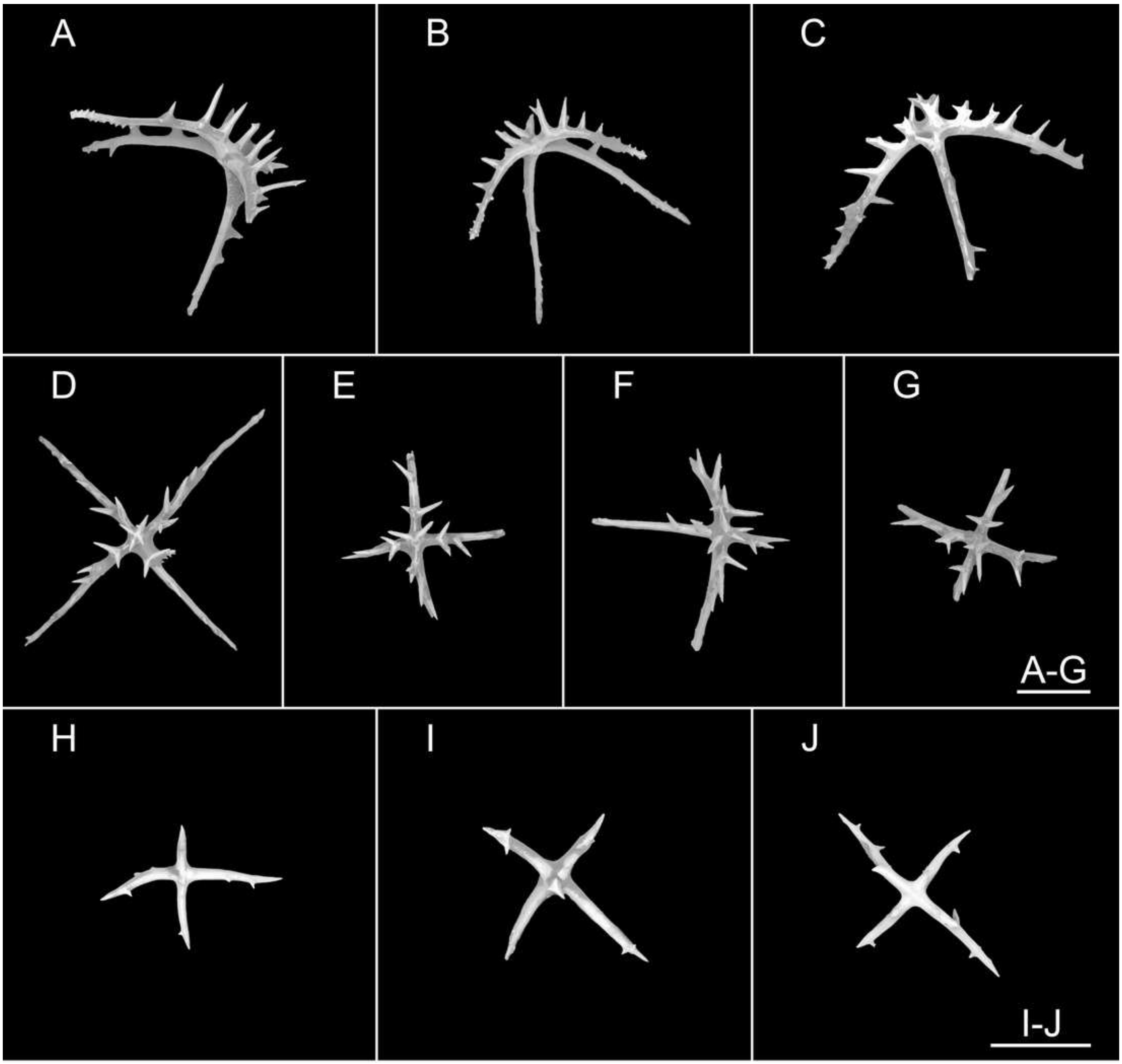

Figure 11

Psychropotes nigrimargaria sp. nov., SEM, holotype (FDZ188-F02).

(A–K) Ossicles from tube feet; (L–N) tentacles. Scale bars: 100 µm.

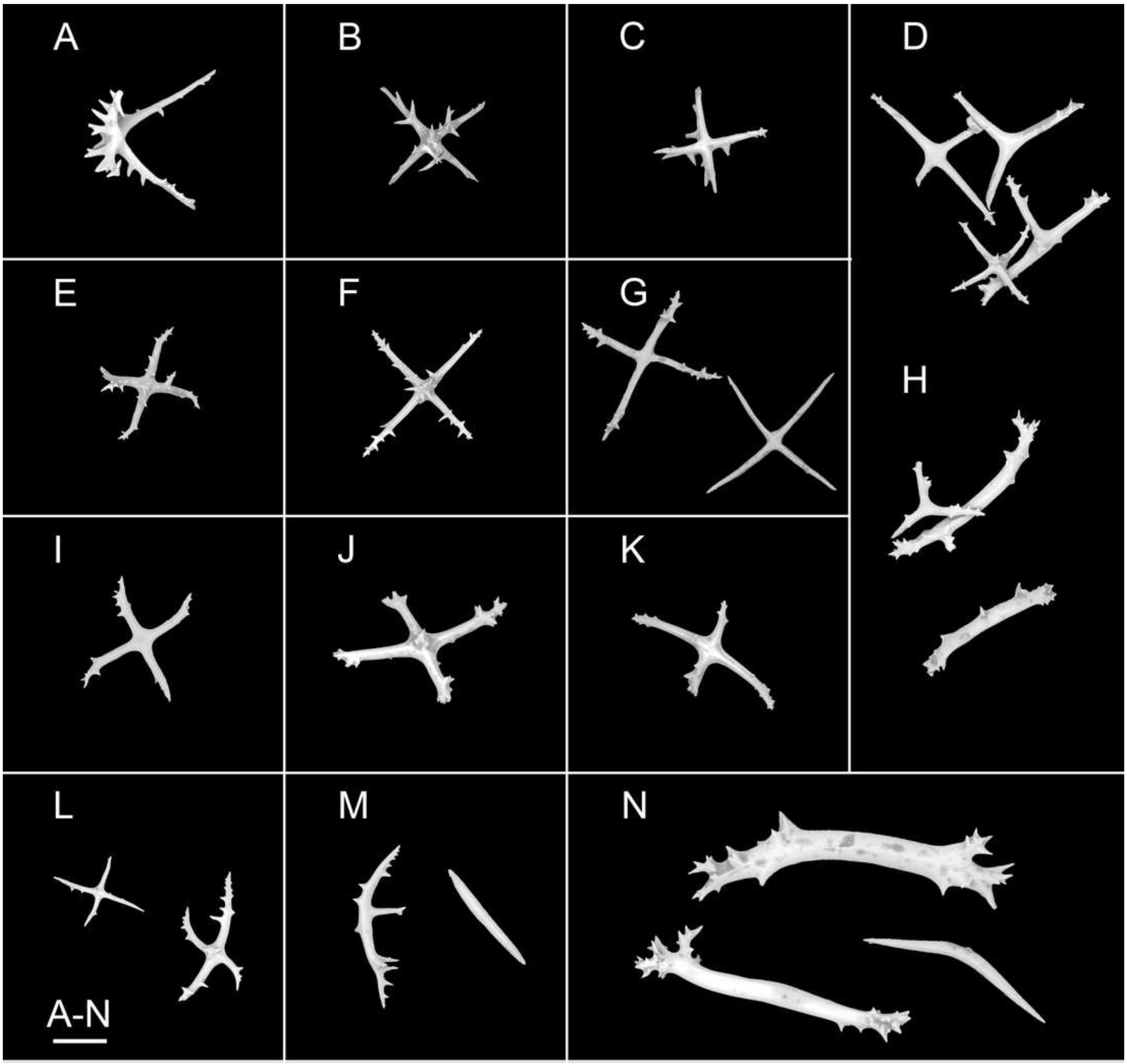

Figure 12

Psychropotes depressa (Théel, 1882) (NIWA164160).

(A) *In situ* images. (B) Specimen after fixation. (C–J) Dorsal ossicles under SEM. Scale bars: (A) the distance between the two laser points is 10cm ; (B) 1 cm; (C–J) 200 μm.

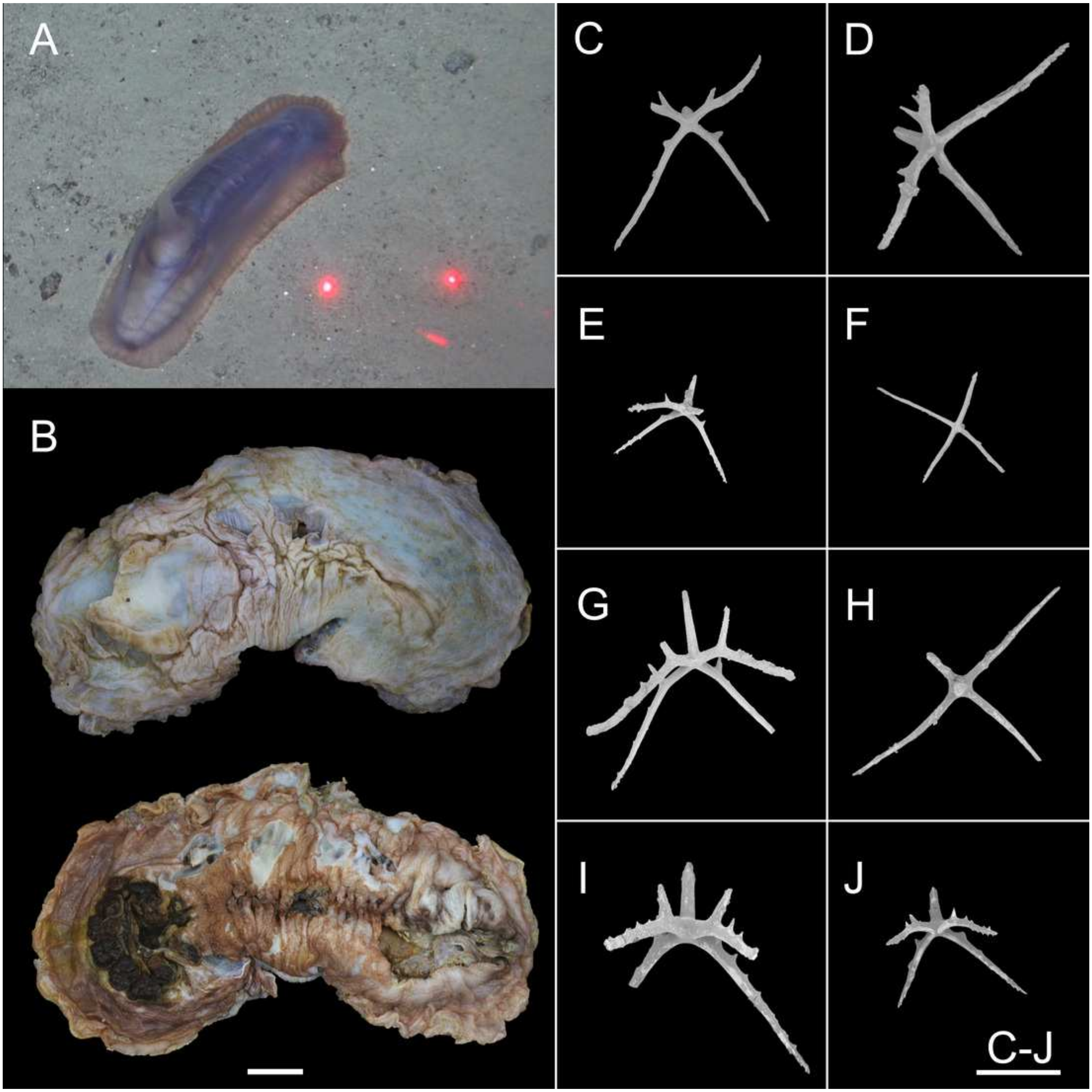
A
B
C
D
E
F
G
H
I
J
C-J

Figure 13

Psychropotes depressa (Théel, 1882), drawing and SEM, (NIWA164160).

(A) Ossicles from dorsal papillae; (B) dorsal body wall; (C) unpaired dorsal appendage; (D) tentacles. Scale bars: 100 µm.

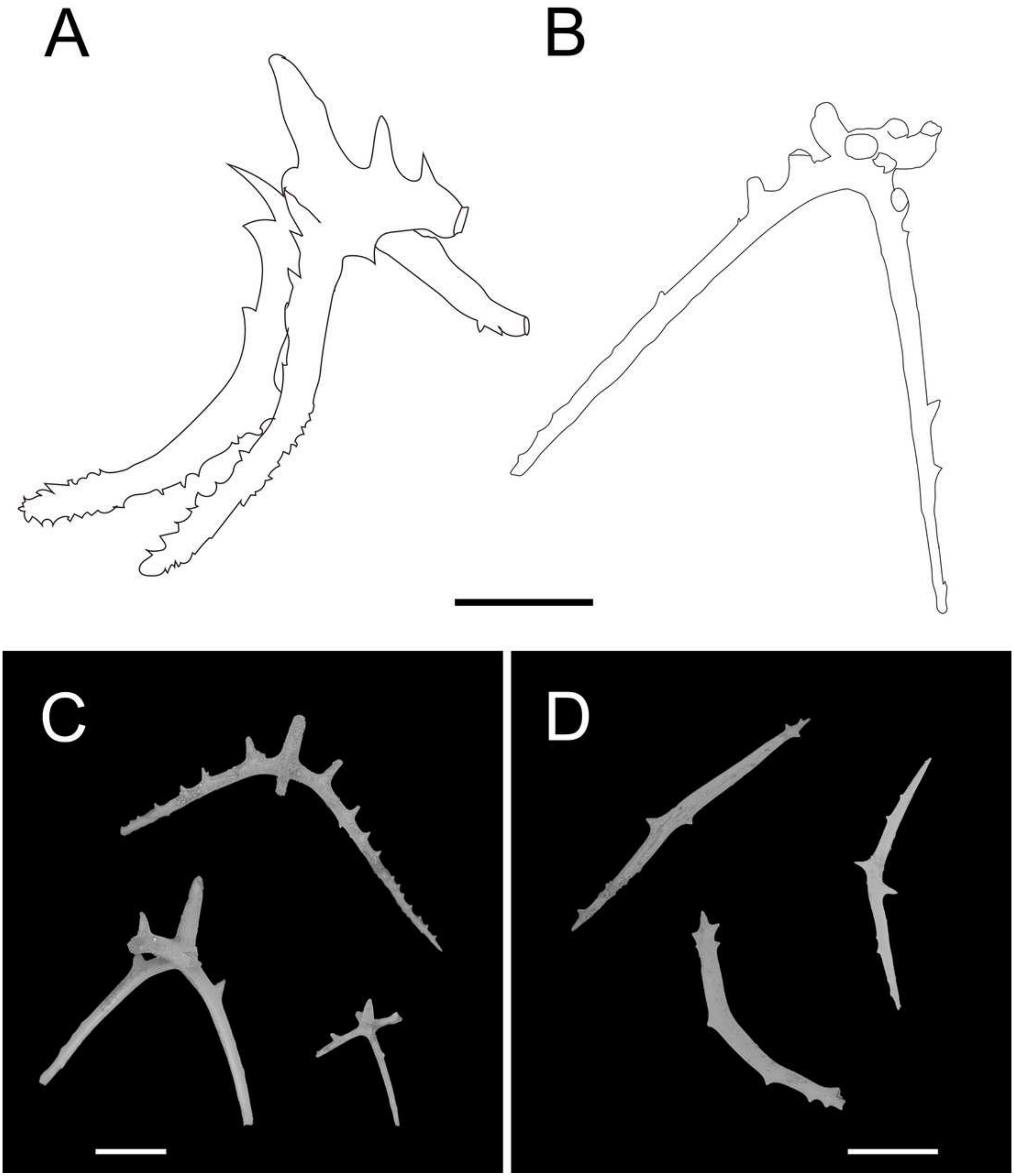
A
B
C
D

Figure 14

Maximum-likelihood (ML) and Bayesian inference (BI) phylogenetic trees based on COI sequences that show phylogenetic relationships among elasipodid species.

Numbers near branches indicate the bootstrap values (BS) from ML and posterior probabilities (PP) of BI, and the asterisk (∗) indicates that the branch is not supported by the BI tree. The sequences of three new species and one new record of *Psychropotes* provided in this study are in red.

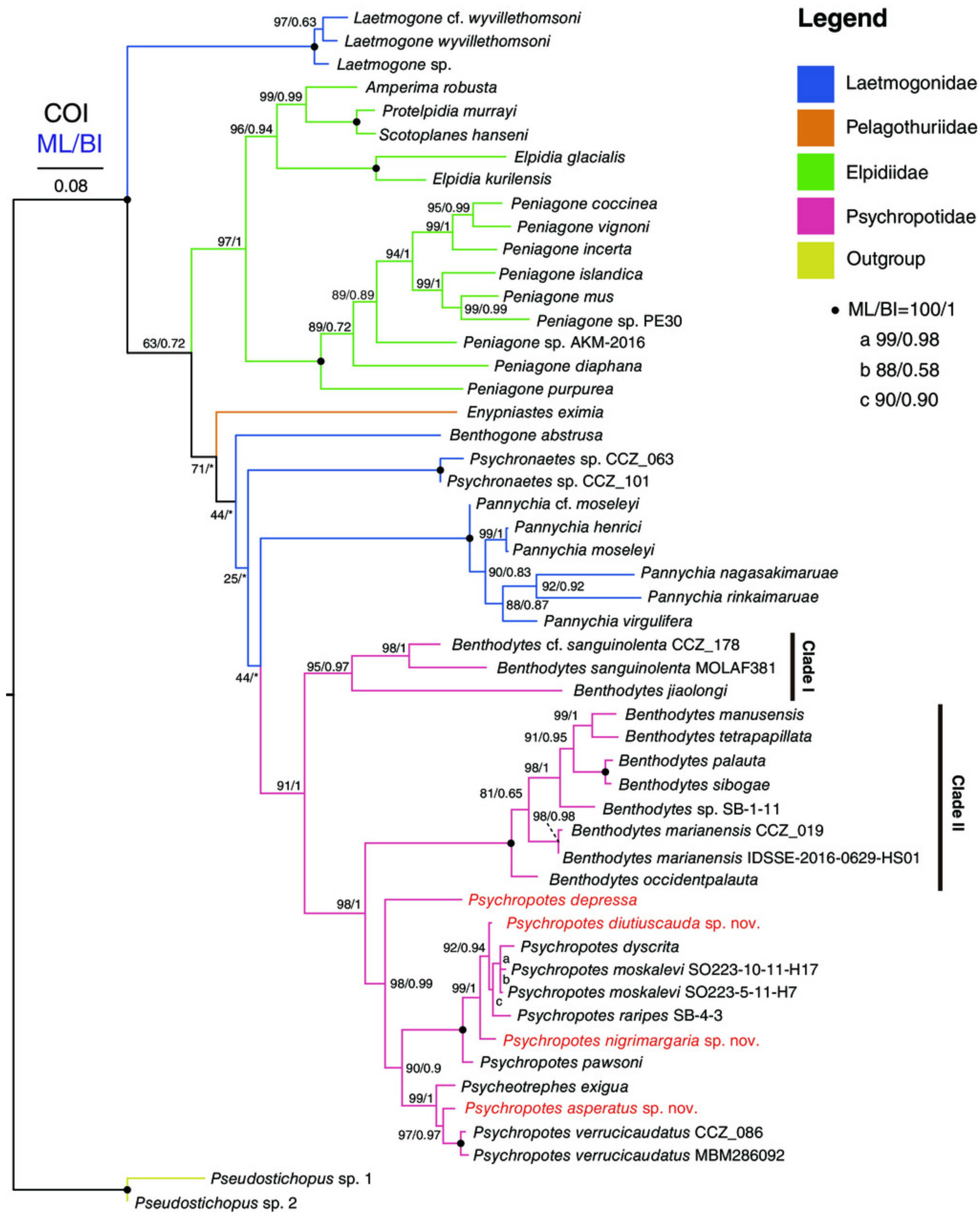
COI
ML/BI
0.08
Legend
Laetmogonidae
Pelagothuriidae
Elpidiidae
Psychropotidae
Outgroup
• ML/BI=100/1
a 99/0.98
b 88/0.58
c 90/0.90
Laetmogone cf. wyvillethomsoni
Laetmogone wyvillethomsoni
Laetmogone sp.
Amperima robusta
Protelpidia murrayi
Scotoplanes hanseni
Elpidia glacialis
Elpidia kurilensis
Peniagone coccinea
Peniagone vignoni
Peniagone incerta
Peniagone islandica
Peniagone mus
Peniagone sp. PE30
Peniagone sp. AKM-2016
Peniagone diaphana
Peniagone purpurea
Enypniastes eximia
Benthogone abstrusa
Psychronaetes sp. CCZ_063
Psychronaetes sp. CCZ_101
Pannychia cf. moseleyi
Pannychia henrici
Pannychia moseleyi
Pannychia nagasakimaruae
Pannychia rinkaimaruae
Pannychia virgulifera
Benthodytes cf. sanguinolenta CCZ_178
Benthodytes sanguinolenta MOLAF381
Benthodytes jiaolongi
Clade I
Benthodytes manusensis
Benthodytes tetrapapillata
Benthodytes palauta
Benthodytes sibogae
Benthodytes sp. SB-1-11
Benthodytes marianensis CCZ_019
Benthodytes marianensis IDSSE-2016-0629-HS01
Benthodytes occidentpalauta
Clade II
Psychropotes depressa
Psychropotes diutiuscauda sp. nov.
Psychropotes dyscrita
Psychropotes moskalevi SO223-10-11-H17
Psychropotes moskalevi SO223-5-11-H7
Psychropotes raripes SB-4-3
Psychropotes nigrimargaria sp. nov.
Psychropotes pawsoni
Psycheotrephes exigua
Psychropotes asperatus sp. nov.
Psychropotes verrucicaudatus CCZ_086
Psychropotes verrucicaudatus MBM286092
Pseudostichopus sp. 1
Pseudostichopus sp. 2
97/0.63
99/0.99
96/0.94
95/0.99
99/1
97/1
94/1
99/1
99/0.99
89/0.89
89/0.72
63/0.72
71/*
44/*
25/*
99/1
90/0.83
92/0.92
88/0.87
44/*
98/1
95/0.97
99/1
91/0.95
98/1
81/0.65
98/0.98
91/1
98/1
92/0.94
98/0.99
99/1
90/0.9
99/1
97/0.97
a
b
c

Figure 15

Maximum-likelihood (ML) and Bayesian inference (BI) phylogenetic trees based on concatenated 16S-COI sequences that show phylogenetic relationships among elasipodid species.

Numbers near branches indicate the bootstrap values from ML and posterior probabilities of BI, and the asterisk (∗) indicates that the branch is not supported by the BI tree. The sequences of three new species and one new record provided in this study are in red.

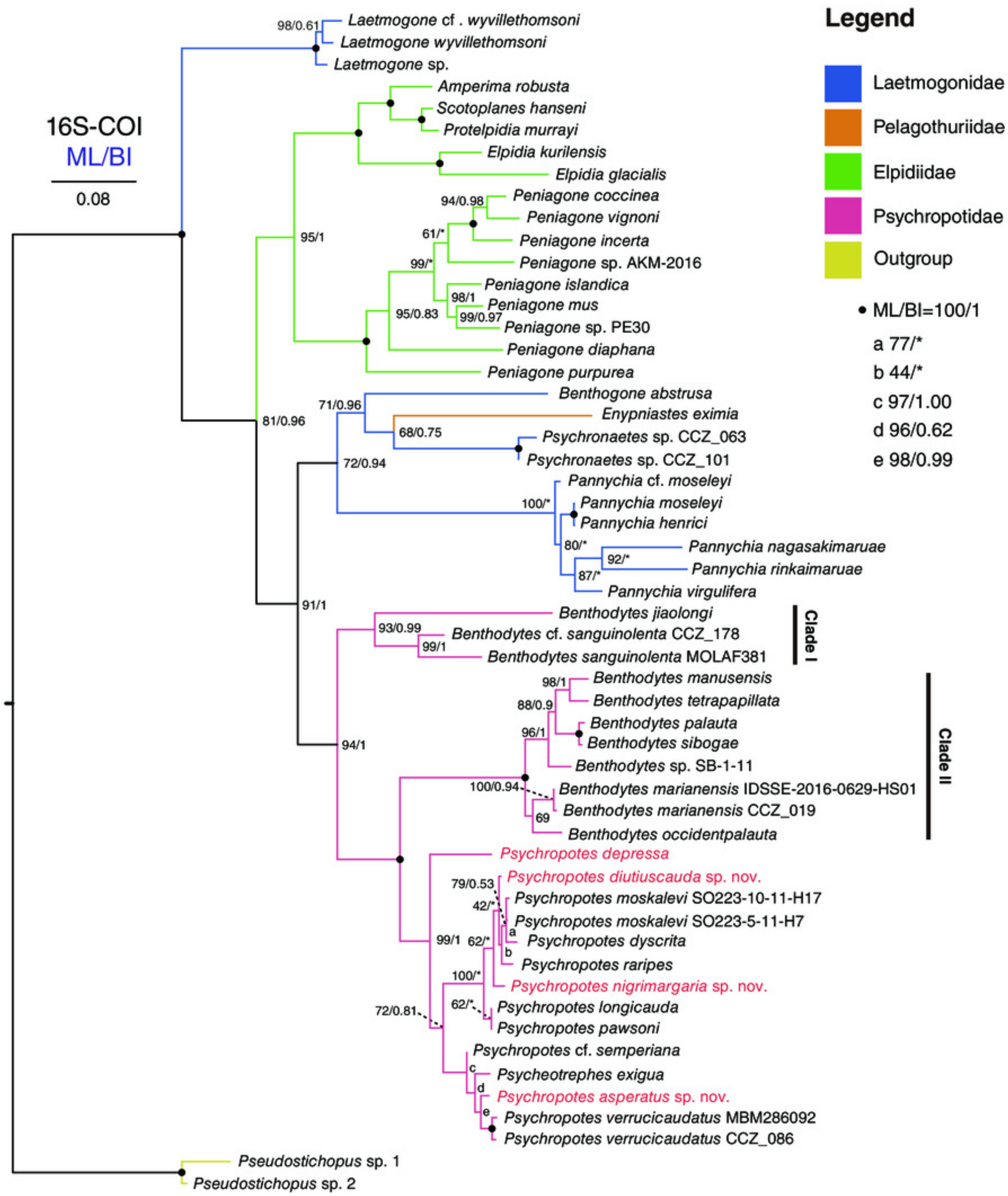
16S-COI
ML/BI
0.08
Legend
Laetmogonidae
Pelagothuriidae
Elpidiidae
Psychropotidae
Outgroup
• ML/BI=100/1
a 77/*
b 44/*
c 97/1.00
d 96/0.62
e 98/0.99
Laetmogone cf . wyvillethomsoni
Laetmogone wyvillethomsoni
Laetmogone sp.
Amperima robusta
Scotoplanes hanseni
Protelpidia murrayi
Elpidia kurilensis
Elpidia glacialis
Peniagone coccinea
Peniagone vignoni
Peniagone incerta
Peniagone sp. AKM-2016
Peniagone islandica
Peniagone mus
Peniagone sp. PE30
Peniagone diaphana
Peniagone purpurea
Benthogone abstrusa
Enypniastes eximia
Psychronaetes sp. CCZ_063
Psychronaetes sp. CCZ_101
Pannychia cf. moseleyi
Pannychia moseleyi
Pannychia henrici
Pannychia nagasakimaruae
Pannychia rinkaimaruae
Pannychia virgulifera
Benthodytes jiaolongi
Benthodytes cf. sanguinolenta CCZ_178
Benthodytes sanguinolenta MOLAF381
Clade I
Benthodytes manusensis
Benthodytes tetrapapillata
Benthodytes palauta
Benthodytes sibogae
Benthodytes sp. SB-1-11
Benthodytes marianensis IDSSE-2016-0629-HS01
Benthodytes marianensis CCZ_019
Benthodytes occidentpalauta
Clade II
Psychropotes depressa
Psychropotes diutiuscauda sp. nov.
Psychropotes moskalevi SO223-10-11-H17
Psychropotes moskalevi SO223-5-11-H7
Psychropotes dyscrita
Psychropotes raripes
Psychropotes nigrimargaria sp. nov.
Psychropotes longicauda
Psychropotes pawsoni
Psychropotes cf. semperiana
Psycheotrephes exigua
Psychropotes asperatus sp. nov.
Psychropotes verrucicaudatus MBM286092
Psychropotes verrucicaudatus CCZ_086
Pseudostichopus sp. 1
Pseudostichopus sp. 2
98/0.61
95/1
94/0.98
61/*
99/*
98/1
99/0.97
95/0.83
81/0.96
71/0.96
68/0.75
72/0.94
100/*
80/*
92/*
87/*
91/1
93/0.99
99/1
98/1
88/0.9
96/1
100/0.94
69
94/1
79/0.53
42/*
62/*
99/1
100/*
62/*
72/0.81

Figure 16

The world distribution of species of Psychropotidae based on OBIS and GBIF data.

(A) *Psychropotes* Théel, 1882. (B) *Benthodytes* Théel, 1882. (C) *Psycheotrephes* Théel, 1882. Species are represented by different colors.

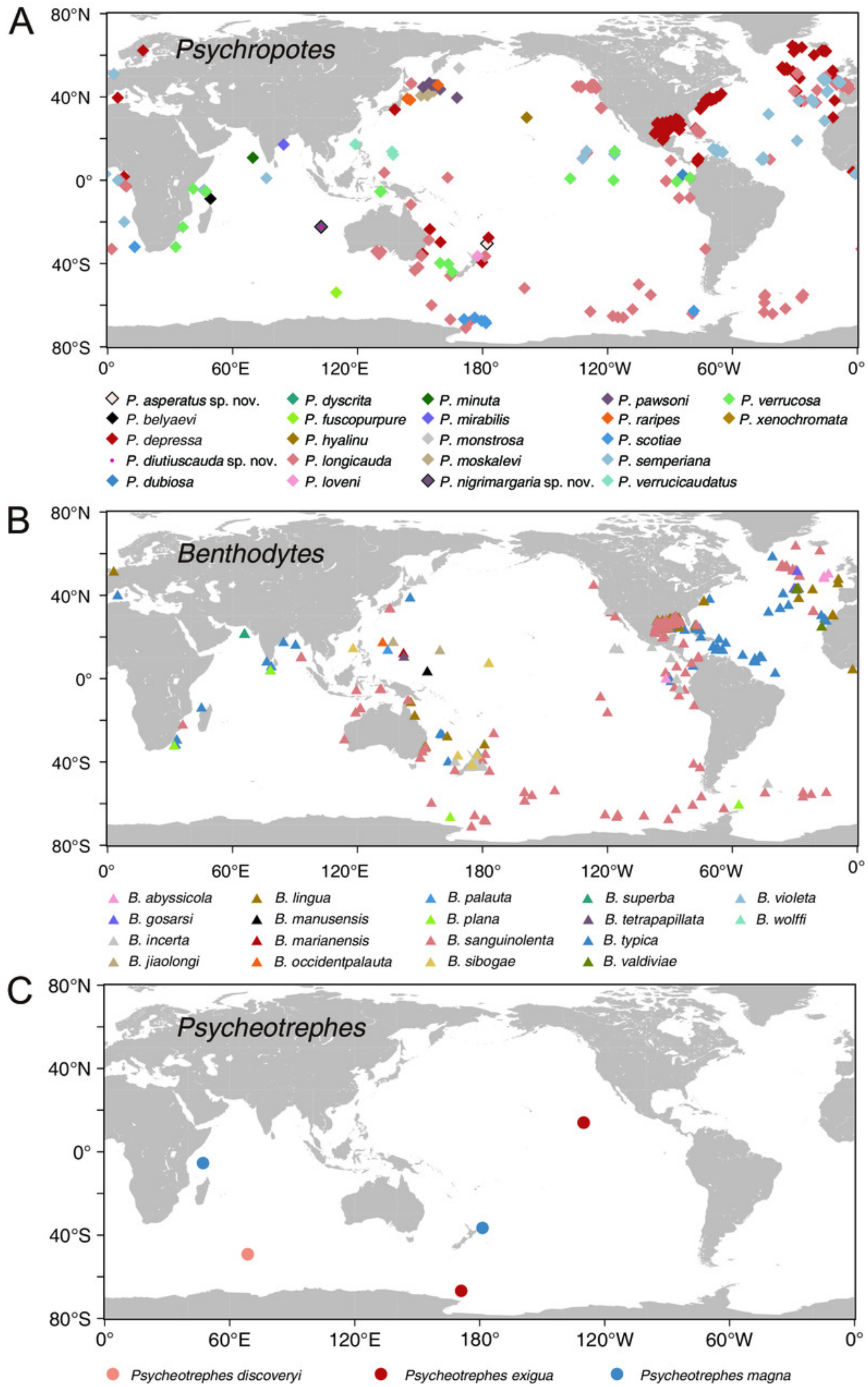
A
Psychropotes
80°N
40°N
0°
40°S
80°S
0°
60°E
120°E
180°
120°W
60°W
0°
P. asperatus sp. nov.
P. belyaevi
P. depressa
P. diutiuscauda sp. nov.
P. dubiosa
P. dyscrita
P. fuscopurpure
P. hyalinu
P. longicauda
P. loveni
P. minuta
P. mirabilis
P. monstrosa
P. moskalevi
P. nigrimargaria sp. nov.
P. pawsoni
P. raripes
P. scotiae
P. semperiana
P. verrucicaudatus
P. verrucosa
P. xenochromata
B
Benthodytes
80°N
40°N
0°
40°S
80°S
0°
60°E
120°E
180°
120°W
60°W
0°
B. abyssicola
B. gosarsi
B. incerta
B. jiaolongi
B. lingua
B. manusensis
B. marianensis
B. occidentpalauta
B. palauta
B. plana
B. sanguinolenta
B. sibogae
B. superba
B. tetrapapillata
B. typica
B. valdiviae
B. violeta
B. wolffi
C
Psycheotrephes
80°N
40°N
0°
40°S
80°S
0°
60°E
120°E
180°
120°W
60°W
0°
Psycheotrephes discoveryi
Psycheotrephes exigua
Psycheotrephes magna

Table 1(on next page)

Interspecific and intraspecific uncorrected p-distances at COI of nine species of *Psychropotes*.

Intraspecific distances are in bold. '–' means no data.

Table 1. Interspecific and intraspecific uncorrected p-distances at COI of nine species of *Psychropotes*.

	1	2	3	4	5	6	7	8	9
1. *P. asperatus* sp. nov.	–								
2. *P. depressa*	9.99%	–							
3. *P. diutiuscauda* sp. nov.	11.33%	12.05%	–						
4. *P. dyscrita*	13.05%	12.81%	2.55%	–					
5. *P. moskalevi*	10.22–11.23%	12.07–13.06%	1.56–2.27%	1.38–2.64%	**0.00–0.82**%				
6. *P. nigrimargaria* sp. nov.	10.41%	12.02%	2.84%	4.47%	3.48–4.40%	–			
7. *P. pawsoni*	10.27%	12.96%	4.30%	6.21%	4.99–5.24%	4.52%	–		
8. *P. raripes*	12.21%	13.01%	2.47%	2.77%	2.47–3.00%	4.85%	4.31%	–	
9. *P. verrucicaudatus*	3.14–3.26%	10.79–11.06%	11.70–12.65%	12.99–13.54%	10.46–12.66%	11.49–12.38%	11.02–11.35%	12.83–12.85%	**0.22–1.23**%

Intraspecific distances are in bold. '–' means no data.